The Journal of Immunology

IκBα Nuclear Export Enables 4-1BB–Induced cRel Activation and IL-2 Production to Promote CD8 T Cell Immunity

Dominique N. Lisiero, Zhang Cheng, Melba M. Tejera, Brandon T. Neldner, Jay W. Warrick, Shelly M. Wuerzberger-Davis, Alexander Hoffmann, M. Suresh and Shigeki Miyamoto

J Immunol published online 14 August 2020
http://www.jimmunol.org/content/early/2020/08/13/jimmunol.2000039

Supplementary Material **http://www.jimmunol.org/content/suppl/2020/08/13/jimmunol.2000039.DCSupplemental**

The Journal of Immunology is published twice each month by The American Association of Immunologists, Inc., 1451 Rockville Pike, Suite 650, Rockville, MD 20852

Print ISSN: 0022-1767 Online ISSN: 1550-6606.

Published August 14, 2020, doi:10.4049/jimmunol.2000039

IκBα Nuclear Export Enables 4-1BB–Induced cRel Activation and IL-2 Production to Promote CD8 T Cell Immunity

Dominique N. Lisiero,* Zhang Cheng,† Melba M. Tejera,‡ Brandon T. Neldner,‡ Jay W. Warrick,*,§ Shelly M. Wuerzberger-Davis,* Alexander Hoffmann,† M. Suresh,‡ and Shigeki Miyamoto*,¶

Optimal CD8 T cell immunity is orchestrated by signaling events initiated by TCR recognition of peptide Ag in concert with signals from molecules such as CD28 and 4-1BB. The molecular mechanisms underlying the temporal and spatial signaling dynamics in CD8 T cells remain incompletely understood. In this study, we show that stimulation of naive CD8 T cells with agonistic CD3 and CD28 Abs, mimicking TCR and costimulatory signals, coordinately induces 4-1BB and cRel to enable elevated cytosolic cRel:IκBα complex formation and subsequent 4-1BB–induced IκBα degradation, sustained cRel activation, heightened IL-2 production and T cell expansion. *Nfkbia*$^{NES/NES}$ CD8 T cells harboring a mutated IκBα nuclear export sequence abnormally accumulate inactive cRel:IκBα complexes in the nucleus following stimulation with agonistic anti-CD3 and anti-CD28 Abs, rendering them resistant to 4-1BB induced signaling and a disrupted chain of events necessary for efficient T cell expansion. Consequently, CD8 T cells in *Nfkbia*$^{NES/NES}$ mice poorly expand during viral infection, and this can be overcome by exogenous IL-2 administration. Consistent with cell-based data, adoptive transfer experiments demonstrated that the antiviral CD8 T cell defect in *Nfkbia*$^{NES/NES}$ mice was cell intrinsic. Thus, these results reveal that IκBα, via its unique nuclear export function, enables, rather than inhibits 4-1BB–induced cRel activation and IL-2 production to facilitate optimal CD8 T cell immunity. *The Journal of Immunology*, 2020, 205: 000–000.

CD 8 T cells are important effectors in immune responses to viral infections and cancer (1–3). Following Ag recognition, along with signaling emanating from the TCR complex and CD28, engagement of additional molecules construct a progressive wave of signaling events to ensure a contextually appropriate response (4). Within this complex signaling environment, dysregulated signals can result in suboptimal responses (4, 5). However, the temporal and spatial regulatory mechanisms that coordinate numerous events necessary for robust CD8 T cell immunity in vivo are incompletely understood.

Members of the TNFR superfamily, such as 4-1BB, OX40, and CD27, provide signals to T cells beyond CD3 and CD28 signaling for optimal cytokine production, survival, and memory formation (4). Unlike CD28, these TNFR superfamily members are expressed at low levels in naive cells and are significantly induced following initial TCR stimulation in vivo (2). Similarly, their ligands are transiently upregulated following inflammatory signaling in professional APC as well as on B and T cells (6). Thus, the coordinated expression of TNFR superfamily members and their ligands tune the dynamics of CD8 T cell signaling and responses. However, whether intracellular signaling pathways are also dynamically modulated to coordinate with their respective receptor systems is unknown.

The NF-κB pathway is a key cell signaling pathway that is rapidly engaged following TCR/CD3, CD28, and TNFR superfamily activation. In mammals, the NF-κB family of transcription factors is composed of five family members, RelA (p65), cRel, RelB, p100/p52, and p105/p50, which form cell- and context-specific

*McArdle Laboratory for Cancer Research, Department of Oncology, University of Wisconsin-Madison, Madison, WI 53705; †Department of Microbiology, Immunology, and Molecular Genetics, Institute for Quantitative and Computational Biosciences and Molecular Biology Institute, University of California, Los Angeles, Los Angeles, CA 90025; ‡Department of Pathobiological Sciences, School of Veterinary Medicine, University of Wisconsin-Madison, Madison, WI 53706; §Department of Biomedical Engineering, University of Wisconsin-Madison, Madison, WI 53705; and ¶University of Wisconsin Carbone Cancer Center, University of Wisconsin-Madison, Wisconsin Institute for Medical Research, Madison, WI 53705

ORCIDs: 0000-0003-3863-2866 (Z.C.); 0000-0003-4278-4045 (B.T.N.); 0000-0002-4801-8897 (J.W.W.); 0000-0002-5607-3845 (A.H.); 0000-0003-1794-3358 (M.S.); 0000-0002-7827-3426 (S.M.).

Received for publication February 20, 2020. Accepted for publication July 20, 2020.

This work was supported in part by National Institutes of Health (NIH) Grants T32 CA157322 and F32 AI112206 to D.N.L., U01 AI124299 and R21 AI118326 to M.S., R01 CA081065 and R56 CA081065 to S.M., a Wisconsin Partnership Program award to J.W.W. and S.M., NIH Small Instrument Grants 1S10RR025483-01 and 1S100OD018202-01, and University of Wisconsin Carbone Cancer Center Support Grant P30 CA014520.

D.N.L., Z.C., M.M.T., B.T.N., and S.M.W.-D. performed experiments. D.N.L., Z.C., M.M.T., B.T.N., and J.W.W. contributed to data analysis. D.N.L., M.M.T., Z.C., B.T.N., S.M.W.-D., A.H., M.S., and S.M. contributed to the study design. M.S. and S.M. provided overall project leadership and supervised the analysis. D.N.L., M.S., and S.M. wrote the manuscript, which was edited and approved by all authors.

Address correspondence and reprint requests to Dr. M. Suresh or Dr. Shigeki Miyamoto, Department of Pathobiological Sciences, School of Veterinary Medicine, University of Wisconsin-Madison, Madison, WI 53706 (M.S.) or University of Wisconsin Carbone Cancer Center, University of Wisconsin-Madison, Wisconsin Institute for Medical Research, Madison, WI 53705 (S.M.). E-mail addresses: sureshm@vetmed.wisc.edu (M.S.) or smiyamot@wisc.edu (S.M.)

The online version of this article contains supplemental material.

Abbreviations used in this article: CC, control chimera; EC, experimental chimera; FVD, Fixable Viability Dye; IP, coimmunoprecipitation; LCMV, lymphocytic choriomeningitis virus; LMB, leptomycin B; NES, nuclear export sequence; PBST, PBS containing 0.2% Tween 20; RNA-seq, RNA sequencing; WT, wild-type.

homo- and heterodimers (7–9). Canonical NF-κB complexes frequently consist of RelA:p50 or cRel:p50 dimers, whereas RelB:p52 dimers represent noncanonical complexes. Normally, canonical dimers are held in stable inactive cytoplasmic complexes by the IκB family of inhibitor proteins, of which the main family member, IκBα, preferentially binds RelA and cRel dimers, but not RelB:p52 dimers (10). Upon stimulation, IκB proteins are phosphorylated and degraded allowing free NF-κB dimers to enter the nucleus. Free, nuclear NF-κB then regulates expression of its target genes to modulate biological processes, including immune and inflammatory responses. RelA and cRel play particularly critical roles in T cell signaling and function (11–15). However, how NF-κB activities are dynamically and spatially regulated specifically during CD8 T cell immune responses remains incompletely understood.

Among the many NF-κB target genes is the *Nfkbia* gene, which encodes the inhibitor IκBα (16, 17). A negative feedback loop of inhibition occurs when newly synthesized IκBα enters the nucleus, removes NF-κB from DNA, and exports inactive NF-κB complexes to the cytoplasm. This latter process is driven by the nuclear export sequence (NES) of IκBα (18–21). IκBβ, another commonly expressed IκB family member, does not have an NES (18, 21). In addition, both RelA:IκBα and cRel:IκBα complexes shuttle between the nucleus and the cytoplasm in unstimulated cells, whereas those complexed with IκBβ do not (19, 22). A classical NES is also present in RelA, but not cRel (23, 24); however, the physiological significance of the nuclear shuttling or nuclear export regulation of NF-κB:IκB complexes in specific biological contexts remains mostly unclear. To begin to address this, we previously created the *Nfkbia*$^{NES/NES}$ mouse model harboring a germline IκBα NES mutation and reported defects in B cell development and secondary lymphoid tissue formation (25). Contrary to B cells, however, T cell development and mature T cell populations in the periphery remained relatively unaffected in *Nfkbia*$^{NES/NES}$ mice. However, it remains unknown whether CD8 T cell activation and functions are disrupted in these mutant mice.

In this study, we investigated *Nfkbia*$^{NES/NES}$ CD8 T cell responses and found that following stimulation of the TCR and costimulatory receptors by means of agonistic Abs against CD3 and CD28, respectively, the expression of inducible TNFR superfamily members occurred in tandem with a temporally timed cRel induction to assemble increased levels of cytosolic cRel:IκBα complexes in newly activated T cells relative to naive cells. These concurrent events set the stage for magnified and sustained cRel activation in CD8 T cells through the engagement of 4-1BB, resulting in heightened IL-2 production and CD8 T cell expansion. However, such a chain of events was disrupted in *Nfkbia*$^{NES/NES}$ CD8 cells because of abnormal accumulation of inactive cRel:IκBα complexes in the nucleus following stimulation with agonistic anti-CD3 and anti-CD28 Abs (referred from here on as "CD3+CD28"). Consequently, *Nfkbia*$^{NES/NES}$ mice displayed defects in CD8 T cell expansion following infection with lymphocytic choriomeningitis virus (LCMV) which induces a well-defined virus-specific T cell response (26, 27). Overall, our findings highlight how IκBα, a major NF-κB inhibitory protein, governs signaling dynamics and CD8 T cell immunity by temporally and spatially regulating critical accessory signaling events necessary for proper T cell immunity.

Materials and Methods

Mice

Nfkbia$^{NES/NES}$ mice were generated as previously described (25). Six- to twelve-week-old littermate *Nfkbia*$^{WT/WT}$ wild-type (WT) and *Nfkbia*$^{NES/NES}$ mice were age and sex matched for all experiments. Male host mice (B6.SJL-*Ptprc*^{a} *Pepc*^{b}/BoyJ, Ly5.1) used for mixed bone marrow were obtained from The Jackson Laboratory (Bar Harbor, ME). *Rel*$^{-/-}$ mice were obtained from Dr. J. Levenson (28) with permission from Dr. H.-C. Liou. The P14 LCMV GP33-specific TCR-transgenic mice on the Ly5.1 background (provided by Dr. R. Ahmed, Emory University) were bred at the University of Wisconsin-Madison. P14 mice were crossed with *Nfkbia*$^{NES/NES}$ mice to generate P14/*Nfkbia*$^{WT/WT}$ and P14/*Nfkbia*$^{NES/NES}$ mice. All experiments were approved and conducted in accordance by the Institutional Animal Care and Use Committee of the University of Wisconsin-Madison. All mice were housed and bred in specific pathogen-free conditions at the University of Wisconsin-Madison.

In vitro T cell stimulation and ELISA

Naive T cells were isolated from spleens using negative selection with the Pan T Cell Isolation Kit II (Miltenyi Biotec) in addition to anti-CD44 microbeads (Miltenyi Biotec). Naive CD8 T cells were isolated from spleens using negative selection with the Naive CD8a^{+} T cell Isolation Kit (Miltenyi Biotec), and purity was confirmed by flow cytometry to be >95% CD8 CD44^{lo} cells. Cells were cultured in RPMI medium supplemented with 10% FBS, 50 μM 2-ME, 1× GlutaMAX (Life Technologies), 100 U/ml penicillin, and 100 μg/ml streptomycin. Cell culture plates were coated with anti-CD3 (clone 17A2; BioXCell) and anti-CD28 (clone 37.51; BioXCell) Abs overnight at 4°C or for 2 h at 37°C. For 4-1BB and OX40 stimulation, soluble anti–4-1BB (clone 3H3; BioXCell) or anti-OX40 (clone OX86; BioXCell) Abs were added at the start of stimulation with anti-CD3 and anti-CD28. For CD27 stimulation, soluble anti-CD27 Ab (clone LG.3A10; eBioscience) was crosslinked with anti-rat and anti-hamster Ig κ L Chain (no. 550336; BD Biosciences) and added at the start of stimulation. For the IL-2 ELISA (eBioscience), cells were cultured in 96-well plates for 48 h and supernatants were collected and frozen at −80°C until ready to assay. ELISA data are represented as the mean ± SEM of at least three technical replicates and significance was determined using an unpaired Student *t* test. Generated *p* values are two-tailed, and $*p < 0.05$, $**p < 0.01$, and $***p < 0.001$ were considered statistically significant. For proliferation assays, splenocytes were stained with 10 μM CFSE (Invitrogen) in RPMI with 10% FBS for 10 min at room temperature. Naive CD8 T cells were then isolated as described above. For cell survival assays, 1×10^6 naive CD8 T cells were stimulated with plate bound 5 μg/ml each of anti-CD3 and anti-CD28 Abs, and soluble anti–4-1BB Ab for 48 h in 24-well plates. Following this initial 48 h, viable cells were quantified by the MACSquant flow cytometer, and 4×10^5 cells were replated in 24-well plates in RPMI media supplemented with 10% FBS, 50 μM 2-ME, 1× GlutaMAX (Life Technologies), 100 U/ml penicillin, and 100 μg/ml streptomycin. Viable cells were quantified by the MACSquant flow cytometer 48 h following replating. For cell survival studies, data are represented as the mean ± SEM of at least three technical replicates and significance was determined using an unpaired Student *t* test. Generated *p* values are two-tailed, and $***p < 0.001$ was considered statistically significant.

EMSA and supershift assay

T cells were lysed in Totex buffer (20 mM HEPES [pH 7.9], 350 mM NaCl, 20% glycerol, 1% NP-40, 1 mM $MgCl_2$, 0.5 mM EDTA, 0.1 mM EGTA, 0.5 mM DTT) with 1× HALT protease inhibitor mixture (Thermo Fisher Scientific) and 1 μM DTT. Cell extracts (6–10 μg) were incubated with 1 μg of poly(dI-dC) and EMSA binding buffer (75 mM NaCl, 15 mM Tris HCl [pH 7.5], 1.5 mM EDTA, 1.5 mM DTT, 7.5% glycerol, 0.3% NP-40, 20 μg/ml BSA) in a total reaction volume of 9 μl for 20 min at 4°C. For supershift assays, 1 μl of each Ab (0.2 μg) for RelA (clone C-20; Santa Cruz Biotechnology), cRel (clone C; Santa Cruz Biotechnology), or RelB (clone C-19; Santa Cruz Biotechnology) was added to cell extracts, with the reaction volume not exceeding 10 μl. One microliter of [^{32}P]-labeled double-stranded oligonucleotides containing the κB site from the Igκ gene (5′-TCAACAGAGGGGACTTTCCGAGAGGCC-3′), the IL-2 gene (5′-GACCAAGAGGGATTTCACCTAAATCCA-3′), or the Oct-1 consensus site (Promega) was added to the reaction and incubated for 20 min at room temperature and spun down at 14,000 RPM prior to sample loading and separation on a 4% native polyacrylamide gel, which was then dried and exposed to film or a storage phosphor screen. A Typhoon Biomolecular Imager (GE Healthcare) and accompanying ImageQuant TL software were used to scan and quantify resulting EMSAs. NF-κB binding was first normalized to Oct-1 binding and fold change was determined. Data are represented as the mean ± SEM of at least three biological replicates and significance was determined using a paired Student *t* test. Generated *p* values are two-tailed, and $*p < 0.05$, $**p < 0.01$, and $***p < 0.001$ were considered statistically significant.

Immunoblotting and immunoprecipitation analyses

Samples were lysed in Totex buffer and normalized by total protein amount before being diluted 1:1 with 2× Laemmli sample buffer and boiled for

10 min. Protein extracts were separated on a 10% SDS-PAGE gel and then transferred to a PVDF membrane (MilliporeSigma). Membranes were blocked in PBS containing 0.2% Tween 20 (PBST) and 5% milk for 1 h. The membrane was then probed with the Abs against RelA (clone C-20; Santa Cruz Biotechnology), RelB (clone C-19; Santa Cruz Biotechnology), cRel (clone C; Santa Cruz Biotechnology), p105/p50 (clone NLS; Santa Cruz Biotechnology), p100/p52 (clone C-5; Santa Cruz Biotechnology), IκBα (clone C-21; Santa Cruz Biotechnology), IκBβ (clone C-20; Santa Cruz Biotechnology), or tubulin (clone DM1A; Calbiochem) diluted in PBST overnight. The following day, membranes were washed three times in PBST and incubated with the secondary anti-rabbit IgG (NA934V; GE Healthcare) or anti-goat IgG Ab (NA931V; GE Healthcare) conjugated to HRP. Membranes were washed three times in PBST and developed using Amersham ECL Western blotting Detection Reagents (GE Healthcare). To detect degradation of IκBα and IκBβ, cells were incubated with the protein synthesis inhibitor, cycloheximide, at 20 μg/ml for 30 min at 37˚C prior to stimulation. For IκBα:NF-κB coimmunoprecipitation (IP) analyses, samples were lysed in IP buffer (20 mM Tris, 250 mM NaCl, 3 mM EDTA, 3mM EGTA, 0.5% NP-40, 1mM DTT, and 1× HALT) for 20 min at 4˚C. Cells were then completely lysed by three cycles of freezing by incubating tubes containing cells in 70% ethanol in dry ice for 2 min and thawing in a 37˚C water bath for 2 min. This was followed by an incubation at 4˚C for 10 min and centrifugation at 14,000 RPM for 10 min at 4˚C. Total protein concentration in lysates was determined and ∼150–200 μg of protein was brought to a final volume of 500 μl in IP buffer. Samples were rotated at 4˚C with 2 μg of anti-IκBα Ab (clone C-21; Santa Cruz Biotechnology) for 1 h. In the meantime, protein A Sepharose beads (GE Healthcare) were equilibrated with IP buffer. Approximately 50 μl of 1:1 equilibrated beads were added to each IP sample. Samples were rotated overnight at 4˚C. Beads were washed with IP buffer three times and then resuspended in 100 μl of Laemmli buffer, boiled for 10 min, and loaded onto a 10% SDS-PAGE gel for analysis by immunoblotting.

Immunofluorescence staining and ImageStream acquisition and analysis

To induce maximal RelA, cRel, and IκBα nuclear localization, naive and activated CD8 T cells and B cells were incubated with 20 ng/ml leptomycin B (LMB) (Cayman Chemical) for 40 min at 37˚C. Activated CD8 T cells were stained with Fixable Viability Dye (FVD) eFluor 780 (eBioscience) prior to fixation. CD8 T cells and B cells were fixed with 4% paraformaldehyde for 10 min and permeabilized with 0.3% Triton X-100 for 30 min. Following permeabilization, cells were stained with anti-RelA (no. D14E12, 1:200; Cell Signaling), anti-cRel (no. SC-71, 1:150; Santa Cruz Biotechnology), or anti-IκBα (no. SC-371, 1:200; Santa Cruz Biotechnology) Abs with 1.5% normal goat serum overnight at 4˚C. The following day, primary Ab was removed and cells were incubated with a goat anti-rabbit secondary Ab directly conjugated to Alexa Fluor 488 (Cell Signaling) in 1.5% normal goat serum for 1 h at 4˚C. Nuclear staining was achieved with 5 μM DRAQ5 (BD Biosciences) for 10 min at 37˚C immediately prior to acquisition. Cells were collected at 60× magnification and the low-speed/high-sensitivity setting using an ImageStream flow cytometer (Amnis ImageStreamX Mk II, two lasers [488 and 642 nm] and six channels [457/45, 533/55, 577/35, 610/30, 702/85, 762/35]). Single, focused, and viable cells were collected based on Area and Aspect Ratio in the brightfield channel, Gradient RMS in the nuclear channel, and exclusion of FVD eFluor 780. Using the IDEAS software package, the "similarity score" was calculated using at least 1500–2000 cells based on positive staining for RelA, cRel, or IκBα and DRAQ5.

Gene expression analysis and RNA sequencing

Naive WT and *Nfkbia*$^{NES/NES}$ CD8 T cells were stimulated with plate bound 5 μg/ml anti-CD3 and 5 μg/ml anti-CD28 Abs with or without soluble anti–4-1BB Ab for 12 h. Cells were lysed in TRIzol reagent (Invitrogen) and frozen at −80˚C until total RNA was extracted with the Direct-zol RNA MiniPrep Plus Kit (Zymo Research). For RNA sequencing (RNA-seq), libraries were generated with the TruSeq Stranded mRNA Library Prep Kit for NeoPrep (Illumina) and sequencing was performed on an Illumina HiSeq 2000.

RNA-seq processing and analysis

Adapter-trimmed reads were aligned to the mouse (mm10) genome using STAR with default parameters (29). Only primary mapped reads with alignment score >30 were selected by using "samtools view" with "–F 2820" and "–q 30" and then input into featureCounts (30) to get counts per gene using GENCODE M6 (GRCm38.p4) annotation. The number of raw reads from sequencing is ∼22 million per sample and the final number of reads after filtering was ∼16 million reads per sample. The average Pearson correlation between biological replicates was ∼0.995 using log2 counts per million reads.

To obtain the final "NES-dependent" gene list, we performed two rounds of differential gene expression analysis by using R package EdgeR (glmFit and glmLRT functions) (31). First, we selected 4-1BB–induced genes by testing between 12 h 4-1BB–stimulated samples (12 h+) against 12 h unstimulated samples (12 h−) ($n = 3$ for each time point) in WT (log2 fold change >1 and false discovery rate [FDR] <0.01). A second test between WT versus NES at 12 h of 4-1BB stimulation was performed to determine NES dependency (log fold change < −0.5 and FDR <0.05). Lastly, by intersecting the genes from this two-round analysis, we divided these genes into three categories: 1) induced in WT but induction is not NES dependent ("NES independent"); 2) induced in WT and induction is NES dependent (NES dependent); 3) not induced in WT and expression is reduced in NES mutant ("NES reduced"). Of these, NES-dependent genes' Ensembl IDs were entered into DAVID 6.8 to perform functional enrichment analysis on KEGG_PATHWAY. The reads per kilobase of transcript per million mapped reads for these genes were normalized to [0.1] range for each gene and then used to produce an expression heatmap. The top 50 induced genes in WT were ranked based on induction fold change in WT and selected after filtering genes with average reads per kilobase of transcript per million mapped reads <3 for WT 12 h−.

Motif enrichment analysis

To study the binding motif enrichment of RelA:p50, cRel:p50, and cRel:cRel (32), position weight matrixes (33) were inputted into HOMER motif discovery software (34) and their occurrence was scanned for in the promoter regions of NES-dependent and NES-independent genes (promoters defined as −1000 bp to 300 bp of TSS). Fisher exact test was performed to calculate the fold enrichment and p value for each motif in NES-dependent against NES-independent genes.

Viral infections

Six- to eight-week-old WT and *Nfkbia*$^{NES/NES}$ mice were infected i.p. with 2×10^5 PFUs of the Armstrong strain of LCMV to induce an acute infection. For reinfection of mixed bone marrow chimeras, LCMV immunized mice were infected i.v. with 2×10^6 PFU of the clone 13 strain of LCMV. Plaque assays on Vero cells were used for quantification of infectious LCMV, as previously described (27).

Flow cytometry and cell staining

Peripheral blood was collected in 4% sodium citrate and mononuclear cells were isolated following density centrifugation with Ficoll Histopaque (Sigma-Aldrich). Single-cell suspensions of mononuclear cells from spleens were obtained using a standard procedure. Approximately 1×10^6 cells were stained per sample. Cells were first stained with FVD eFluor 780 or eFluor 450 (eBioscience), followed by staining with MHC class I tetramers specific for the LCMV epitope H2-D^b NP$_{396–404}$ and/or H2-D^b GP$_{33–41}$ (National Institutes of Health Tetramer Facility) and Abs against cell surface markers, CD8 (clone 53-6.7; BD Biosciencies), CD44 (clone IM7; BD Biosciencies), IFN-γ (clone XMG1.2; BD Biosciencies), CD62L (clone MEL-14; BD Biosciencies), KLRG1 (clone 2F1; BD Biosciencies), Ly5.1 (clone A20; BD Biosciencies), Ly5.2 (clone 45.2; BD Biosciencies), Thy1.1 (clone OX-7; BD Biosciencies), and Thy1.2 (clone 53-2.1; BD Biosciencies). Cells were then fixed with 4% paraformaldehyde. For intracellular cytokine staining, splenocytes were stimulated ex vivo with LCMV epitope NP$_{396–404}$ (200 ng/ml), Golgi Plug (BD Biosciences), and IL-2 (2.5 ng/ml) for 5 h at 37˚C. Following incubation, cells were stained with cell surface markers first, fixed, and permeabilized using the Intracellular Fixation and Permeabilization Buffer Set (eBioscience) and then stained with anti–IFN-γ Ab. For LCMV studies, data are represented as the mean ± SEM of biological replicates and significance was determined using an unpaired Student t test. Generated p values are two-tailed, and $*p < 0.05$, $**p < 0.01$, and $***p < 0.001$ were considered statistically significant.

Generation of mixed bone marrow chimeras

Bone marrow cells were obtained from the femurs and tibias of host strain male (B6.SJL-*Ptprc*^{a} *Pepc*^{b}/BoyJ, Ly5.1) mice, WT (Ly5.2), and *Nfkbia*$^{NES/NES}$ mice (Ly5.2). An equal number of bone marrow cells from host strain mice (Ly5.1) was mixed with an equal number of cells from either WT (Ly5.2) or *Nfkbia*$^{NES/NES}$ (Ly5.2) mice. A total of 8×10^6 cells were adoptively transferred into lethally irradiated (450 rad × 2) male host mice (Ly5.1). Following reconstitution, host mice were given neomycin (25 μg/ml) and Polymyxin B (13 μg/ml) in drinking water every other day

for 6 wk. Reconstitution of the hematopoietic compartment was assessed 6 wk following reconstitution by analysis of peripheral blood. Mice were infected with LCMV (Armstrong strain) 1 wk later.

P14/Nfkbia$^{WT/WT}$ and P14/Nfkbia$^{NES/NES}$ adoptive cell transfer assay

For P14 adoptive transfer studies, naive CD8 T cells were purified from P14/*Nfkbia*$^{WT/WT}$ and P14/*Nfkbia*$^{NES/NES}$ mice spleens and 10^4 cells of the appropriate genotype were transferred into recipient mice (B6.PL-*Thy1*^{a}/CyJ; Jackson Laboratory). Mice were infected with LCMV (Armstrong strain) 24 h later as above.

Results

IκBα NES is not required for acute NF-κB activation and proliferation in CD3+CD28-stimulated CD8 T cells

To begin to analyze the activation and functional status of T cells in *Nfkbia*$^{NES/NES}$ mice (25), we first investigated the responses of naive splenic T cells to TCR and costimulatory CD28 signaling by stimulating them on culture plates coated with CD3+CD28. The amounts of Abs used were based on preliminary titration studies (data not shown). EMSA analysis demonstrated that basal and CD3+CD28-induced NF-κB activities were partially reduced in *Nfkbia*$^{NES/NES}$ T cells relative to *Nfkbia*$^{WT/WT}$ (WT) littermate control cells (Supplemental Fig. 1A). To specifically investigate the impact of mutant IκBα on CD8 T cells, naive splenic CD8 T cells were analyzed as above. We evaluated the 2 h time point to examine acute CD3+CD28-induced activation potential and further performed supershift assays to decipher which of the NF-κB subunits was involved. Basal NF-κB activity, primarily composed of RelA, was significantly reduced in *Nfkbia*$^{NES/NES}$ CD8 cells relative to WT counterparts (Fig. 1A). Reduced basal NF-κB activity suggested the possibility that expression of NF-κB–regulated NF-κB family members might be reduced in *Nfkbia*$^{NES/NES}$ CD8 T cells as in the case with splenic mutant B cells (25), which was confirmed by Western blot analysis showing reduced expression of cRel, RelB, p105/p50, and p100, but not RelA (Fig. 1B). IκBα expression was slightly increased, whereas IκBβ expression was slightly reduced in *Nfkbia*$^{NES/NES}$ cells, as was the case in mutant splenic B cells (25). Despite these expression differences of NF-κB and IκB proteins, activation of both RelA and cRel complexes following CD3+CD28 stimulation was not significantly inhibited in the *Nfkbia*$^{NES/NES}$ CD8 T cells (Fig. 1A). Stimulation of *Nfkbia*$^{NES/NES}$ and WT CD8 T cells with CD3+CD28-induced comparable levels of 1) IL-2R α-chain (CD25) and TNFR family member (4-1BB, CD27, OX40) expression, as analyzed by flow cytometry (Fig. 1C); 2) IL-2 secretion, as assessed by ELISA with *Rel*$^{-/-}$ CD8 T cells serving as a control (Fig. 1D); and 3) cell proliferation, as measured with a CFSE dilution assay (Fig. 1E). Thus, contrary to B cells whose maturation, activation and proliferation were significantly defective in *Nfkbia*$^{NES/NES}$ mice (25), the IκBα NES was not necessary for optimal acute CD3+CD28-induced NF-κB activation, activation marker expression, IL-2 secretion, or proliferation in CD8 T cells.

IκBα NES mutation causes 4-1BB signaling defects and functional deficits in CD8 T cells

Proper T cell responses require signaling through not only TCR activation but also additional costimulatory signals (4). Because 4-1BB was expressed at low to undetectable levels in naive cells, but was robustly induced relative to other TNFR family members in both WT and *Nfkbia*$^{NES/NES}$ CD8 T cells (Fig. 1C), we next focused our analyses on 4-1BB signaling. Stimulation of naive CD8 T cells with an agonistic 4-1BB Ab elicited no measurable NF-κB signaling (data not shown). Next, to measure the impact of the NES mutation on 4-1BB signaling, we stimulated naive CD8 T cells with CD3+CD28 Abs in the presence or absence of 4-1BB Ab. We reasoned that 4-1BB would be induced in CD3+CD28-activated CD8 T cells, which would then enable stimulation via the 4-1BB Ab, simulating the dynamics of naive CD8 T cell stimulation by APC (35). Stimulation with CD3+CD28+4-1BB Abs activated both cRel and RelA complexes in WT T cells (Fig. 2A), but the dominant NF-κB complexes shifted from RelA in naive cells activated by CD3+CD28 to cRel in CD3+CD28+4-1BB–stimulated CD8 T cells (Fig. 2B). In striking contrast, activation of RelA and cRel in *Nfkbia*$^{NES/NES}$ cells stimulated with 4-1BB was significantly reduced relative to WT controls and the impact of inhibition was greater for cRel than RelA (an average of 2.3-fold versus 1.5-fold, respectively) (Fig. 2B). Similar differences were also evident at 12 h of CD3+CD28+4-1BB stimulated T cells (Supplemental Fig. 2A). Although certain members of the TNFR superfamily, such as CD40, can strongly activate noncanonical NF-κB (RelB:p52 complex) in B cells (Supplemental Fig. 2B) (36), supershift analyses of 4-1BB-stimulated WT and *Nfkbia*$^{NES/NES}$ CD8 T cells revealed the lack of detectable RelB complexes (Supplemental Fig. 2C). In addition, whereas the processing of the precursor protein p100 to its active p52 form was nearly completely induced by CD40 engagement in WT and *Nfkbia*$^{NES/NES}$ B cells (Supplemental Fig. 2D), the majority of p100 remained unprocessed in 4-1BB-stimulated CD8 T cells of both genotypes (Supplemental Fig. 2E). Thus, activation of only canonical NF-κB complexes was significantly inhibited in 4-1BB-stimulated *Nfkbia*$^{NES/NES}$ CD8 T cells.

The change in cRel dominance of activation following 4-1BB stimulation in WT CD8 T cells (Fig. 2B) correlated with significantly larger amounts of IL-2 production in response to CD3+CD28+4-1BB stimulation in comparison with CD3+CD28 alone (Fig. 2C). 4-1BB-induced IL-2 production was significantly defective in *Nfkbia*$^{NES/NES}$ CD8 T cells, approaching the level of the CD3+CD28 alone condition (Fig. 2C). Furthermore, upregulation of CD25 (IL-2Rα) by CD3+CD28+4-1BB stimulation, which was again much higher than that induced by CD3+CD28, was also significantly reduced in *Nfkbia*$^{NES/NES}$ CD8 T cells (Fig. 2D). The level of phosphorylated STAT5A (pY694) downstream of CD25 signaling under CD3+CD28+4-1BB stimulation in WT T cells was reduced in *Nfkbia*$^{NES/NES}$ cells, which was similar to that detected in similarly stimulated *Rel*$^{-/-}$ cells (Fig. 2E, right). Thus, the CD25 induction defect in the mutant cells likely stemmed from reduced feed forward signaling mediated by IL-2 (37). Moreover, exposure of naive *Nfkbia*$^{NES/NES}$ CD8 T cells to CD3+CD28 and agonistic Abs to OX40 or CD27 also demonstrated defective IL-2 production (Fig. 2F) and CD25 expression (for OX40 stimulation) (Fig. 2G). These results suggested that *Nfkbia*$^{NES/NES}$ CD8 T cell defects were not limited only to 4-1BB but were shared by other TNFR superfamily members.

Based on the above results, we expected that CD8 T cell proliferation in response to CD3+CD28+4-1BB stimulation would be significantly reduced in *Nfkbia*$^{NES/NES}$ CD8 T cells relative to the WT cells. However, although both WT and mutant cells stimulated with CD3+CD28+4-1BB proliferated more than CD3+CD28 stimulation alone, *Nfkbia*$^{NES/NES}$ CD8 T cells proliferated similarly to the WT cells under the same conditions (Fig. 2H). We, therefore, next considered the possibility of higher IL-2 secretion induced by 4-1BB stimulation in WT CD8 T cells relative to mutant cells affecting cell survival. To test this, CD8 T cells were first stimulated by CD3+CD28+4-1BB for 48 h and then cultured for an additional 48 h without any stimuli (see Supplemental

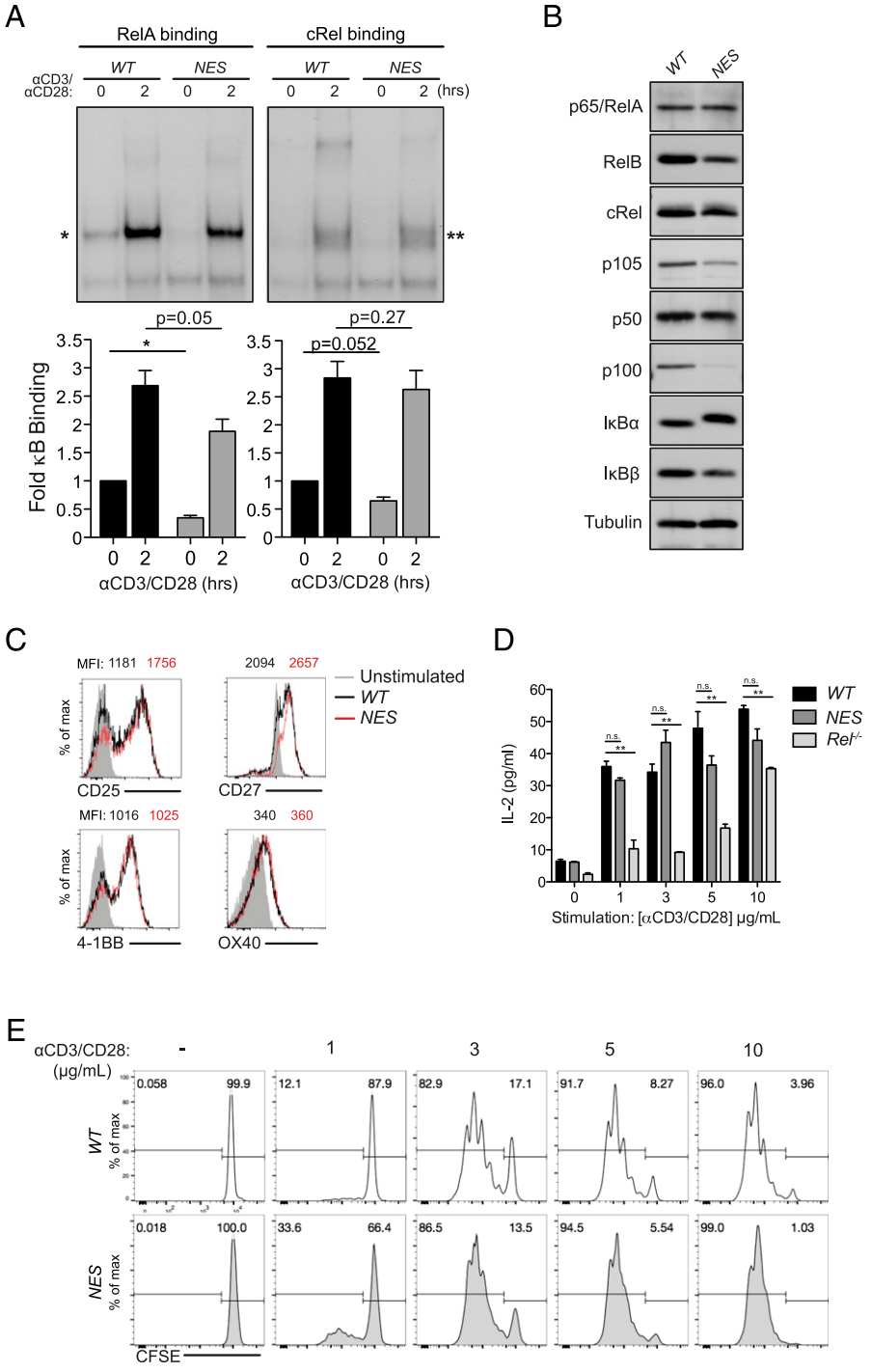

FIGURE 1. IκBα NES is not necessary for efficient CD3+CD28-induced NF-κB activation and proliferation in CD8 T cells. (**A**) Naive *Nfkbia*$^{WT/WT}$ (WT) and *Nfkbia*$^{NES/NES}$ (NES) T cells were stimulated with 5 μg/ml each anti-CD3 and anti-CD28 Abs and cell lysates were prepared. Supershift EMSA analysis with anti-cRel and anti-RelA Abs was used to detect RelA and cRel complexes, respectively. Below, quantification of RelA (left, single asterisk) and cRel (right, double asterisks) binding, relative to unstimulated WT T cells and normalized to Oct-1 binding, is shown as fold change in comparison with unstimulated samples from three independent experiments with the mean ± SEM with statistical significance at $*p < 0.05$ or as indicated. (**B**) Naive CD8 T cells were purified from WT and *Nfkbia*$^{NES/NES}$ spleens and total cell extracts were made. Immunoblot analysis of indicated NF-κB and IκB family members is shown with anti-tubulin as a loading control. (**C**) Naive WT and *Nfkbia*$^{NES/NES}$ CD8 T cells were stimulated with 5 μg/ml each of anti-CD3 and anti-CD28 Abs for 24 h. Cells were analyzed by flow cytometry with unstimulated CD8 T cells shown in shaded gray in each histogram. Median fluorescence intensity (MFI) of WT (black) and *Nfkbia*$^{NES/NES}$ (red) CD8 T cells is shown on top of each histogram. Data are representative of experiments performed independently at least three times. (**D**) WT, *Nfkbia*$^{NES/NES}$, and *Rel*$^{-/-}$ CD8 T cells stimulated for 48 h with 5 μg/ml anti-CD3 and anti-CD28 Abs. Supernatants were analyzed by ELISA for IL-2. Data are the mean ± SEM of three technical replicates with statistical significance at $*p < 0.05$, $**p < 0.01$ and is representative of experiments performed independently at least three times. (**E**) Naive WT and *Nfkbia*$^{NES/NES}$ CD8 T cells were labeled with CFSE and stimulated with the indicated concentrations of anti-CD3 and anti-CD28 Abs for 72 h. Percentages of divided cells are shown. Data are representative of experiments performed independently at least five times.

Fig. 2F for schematic). The recovery of *Nfkbia*$^{NES/NES}$ CD8 T cells was less than 50% of WT cells (Fig. 2I). When a CD25 blocking Ab was included during the first 48 h activation phase to block IL-2 signaling, cell recovery was nearly completely eliminated for both WT and *Nfkbia*$^{NES/NES}$ T cells (Fig. 2I). Thus, IL-2 signaling was required for the accumulation of activated CD8 T cells upon withdrawal of activation signals. Based on these results, we propose that a major function of secreted IL-2 and CD25 signaling in response to 4-1BB stimulation was to promote survival and continued proliferation of activated CD8 T cells. Perhaps, this phenomenon reflects programmed proliferation and accumulation of activated CD8 T cells, following withdrawal of TCR signaling (38). This aspect of CD8 T cell biology was significantly defective in *Nfkbia*$^{NES/NES}$ CD8 T cells.

IκBα NES is necessary for CD3+CD28 induced cytoplasmic localization of IκBα:cRel complexes to enable efficient 4-1BB signaling

Given that the NES of IκBα promotes its own cytoplasmic localization with its associated NF-κB proteins, in particular cRel (25), we next examined subcellular localization of IκBα, RelA, and cRel in naive versus CD3+CD28-stimulated *Nfkbia*$^{NES/NES}$ and WT CD8 T cells. After fixation, permeabilization and staining with appropriate Abs against these proteins (see *Materials and*

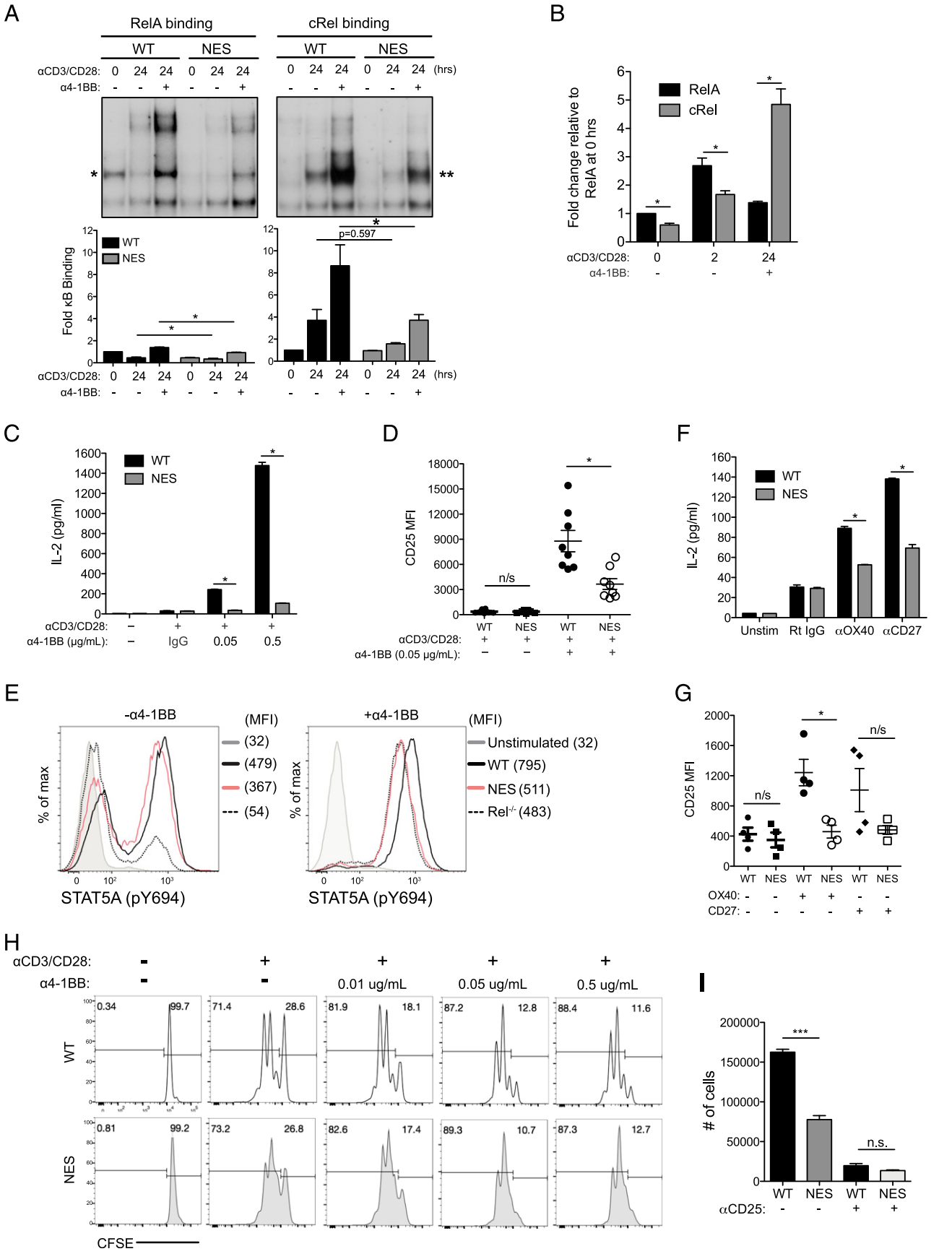

FIGURE 2. IκBα nuclear export culminates in 4-1BB signaling defects in *Nfkbia*$^{NES/NES}$ CD8 T cells. (**A**) Naive WT and *Nfkbia*$^{NES/NES}$ CD8 T cells were stimulated for 24 h with 5 μg/ml anti-CD3 and anti-CD28 Abs with or without 0.05 μg/ml anti–4-1BB Ab. Supershift analysis using anti-cRel and anti-RelA Abs was performed to detect RelA (left, single asterisk) and cRel (right, double asterisks) complexes, respectively. Below, quantification of indicated complexes is shown as fold change in comparison with unstimulated samples and normalized to Oct-1 binding. Data *(Figure legend continues)*

Methods), we used ImageStream flow cytometry and the IDEAS software to calculate a log transformed Pearson correlation coefficient between the pixel values of two images to derive a similarity score (39). We used DRAQ5 nuclear stain along with NF-κB/IκBα staining to obtain similarity scores such that a higher similarity score denoted higher nuclear localization of the protein of interest. We further employed the nuclear export inhibitor, LMB (40), as a control to demonstrate maximal nuclear localization of NF-κB and IκBα proteins. We first tested the utility of this assay using splenic B cells isolated from WT and *Nfkbia*$^{NES/NES}$ hosts. The similarity scores for IκBα and cRel were higher in *Nfkbia*$^{NES/NES}$ B cells compared with WT cells, which were similar to those induced by LMB in WT cells (Supplemental Fig. 3). However, RelA in both WT and mutant cells showed lower similarity scores than LMB conditions. These results are consistent with the NES mutant IκBα causing nuclear localization of associated cRel, but not RelA, complexes, as reported previously (25).

Having validated the assay, we next evaluated subcellular localization of IκBα, RelA, and cRel in naive WT and *Nfkbia*$^{NES/NES}$ CD8 T cells. Analysis of fluorescence imaging indicated that IκBα is largely cytoplasmic in T cells of both genotypes (Fig. 3A, IκBα, upper). Correspondingly, the similarity scores for IκBα in both genotypes were similar and lower than that induced by LMB treatment in WT cells (Fig. 3A, IκBα, lower). The similarity score for RelA in *Nfkbia*$^{NES/NES}$ CD8 T cells was slightly higher than for WT cells but was still much lower than that induced by LMB (Fig. 3A, RelA, lower). For cRel, the similarity score was slightly higher in the mutant cells than WT cells and similar to that increased with LMB treatment in WT cells (Fig. 3A, cRel, lower). Following CD3+CD28 stimulation, expression of not only TNFR family members (Fig. 1C) but also cRel and p50 increased in WT CD8 T cells (Fig. 3B), which was accompanied by increased formation of IκBα/cRel complexes (Fig. 3C). In addition, IκBα and RelA levels were slightly reduced in activated WT cells (Fig. 3B). Now, LMB treatment of CD3+CD28-activated WT CD8 T cells demonstrated a greater increase in the similarity scores in both IκBα and cRel, similar to RelA, relative to those in naive cells (Fig. 3A, 3D, compare WT ± LMB). In *Nfkbia*$^{NES/NES}$ CD8 T cells, cRel and p50 levels also increased with a further reduction in RelA, but not IκBα (Fig. 3B); IκBα and cRel, but not RelA, displayed high similarity scores that approached those scores induced by LMB in WT cells (Fig. 3D, *NES*). These results suggested that newly formed IκBα/cRel complexes in activated T cells were mislocalized to the nucleus in *Nfkbia*$^{NES/NES}$ CD8 T cells, whereas RelA remained cytoplasmic. Accordingly, 4-1BB stimulation of CD3+CD28-activated CD8 T cells caused rapid IκBα degradation in WT cells but much less so in the mutant cells (Fig. 3E). Degradation of IκBβ was barely detectable in both WT and mutant cells. This 4-1BB–induced resistance of IκBα to degradation (due to nuclear accumulation) could explain the significant cRel activation defects observed in *Nfkbia*$^{NES/NES}$ CD8 T cells (Fig. 2A, 2B).

IκBα nuclear export is required for inducing a 4-1BB–mediated NF-κB transcriptional program in CD8 T cells

The biochemical and functional data thus far suggested that a 4-1BB–induced transcriptional program would likely be altered in *Nfkbia*$^{NES/NES}$ CD8 T cells. To define a 4-1BB–induced transcriptional program that requires proper IκBα nuclear export in CD8 T cells, we next performed RNA-seq analyses on WT and *Nfkbia*$^{NES/NES}$ CD8 T cells stimulated with CD3+CD28 with or without 4-1BB stimulation (Fig. 4A). We chose a 12 h time point for analysis to capture early changes induced by 4-1BB signaling as 4-1BB mediated disruption of NF-κB signaling was already evident at this time point (Supplemental Fig. 2A). Stimulation of WT CD8 T cells with CD3+CD28+4-1BB altered expression of a set of up- and downregulated genes relative to CD3+CD28 alone (Fig. 4B, left). Moreover, analysis of similarly stimulated *Nfkbia*$^{NES/NES}$ CD8 T cells revealed three distinct groups of genes (Fig. 4C): 1) NES-independent genes induced by 4-1BB in WT cells and similarly in *Nfkbia*$^{NES/NES}$ (110 genes); 2) NES-dependent genes induced by 4-1BB in WT cells but less induced in *Nfkbia*$^{NES/NES}$ (88 genes); and 3) NES-reduced genes not induced by 4-1BB in WT cells but reduced in *Nfkbia*$^{NES/NES}$ (114 genes) (Fig. 4C). Of these, the NES-dependent category was of particular interest because these genes were candidates whose transcriptional programs were controlled by IκBα nuclear export in response to 4-1BB stimulation over CD3+CD28 alone. Kyoto Encyclopedia of Genes and Genomes pathway analysis of the NES-dependent category revealed an enrichment of pathways such as the TNF and Jak-STAT signaling pathways and processes such as cytokine signaling (Fig. 4D). A ranking of the most upregulated genes by 4-1BB based on their fold induction in WT CD8 T cells revealed those relevant to 4-1BB biology, such as *Icam1*, *Fas*, and *Jun* (Fig. 4E). This ranking also demonstrated that *Il2* was the second most highly induced gene. This corroborates our previous finding that IL-2 secretion was significantly reduced in 4-1BB–stimulated *Nfkbia*$^{NES/NES}$ CD8 T cells (Fig. 2C).

To assess whether NES-dependent genes were under the control of the NF-κB pathway, in particular, cRel complexes, as our previous biochemical and imaging data suggest (Figs. 2, 3), promoter regions of these genes were tested for the enrichment of NF-κB consensus motifs for RelA:p50, cRel:p50, and cRel:cRel complexes (32, 33). We found the greatest enrichment of cRel:p50

plotted are the mean ± SEM and includes three independent experiments with statistical significance at $*p < 0.05$. (**B**) Absolute RelA and cRel binding levels in Figs. 1A and 2A relative to the absolute RelA binding level at 0 h (Fig. 2A) and normalized to Oct-1 binding are shown with SEM and statistical significance at $*p < 0.05$. (**C**) Naive WT and *Nfkbia*$^{NES/NES}$ CD8 T cells were stimulated for 48 h with 5 μg/ml anti-CD3 and anti-CD28 Abs with or without increasing concentrations of anti–4-1BB Ab or normal rat IgG control. Supernatants were analyzed by ELISA for IL-2. Data are the mean ± SEM of three technical replicates and $*p < 0.05$ and representative of three independent experiments. (**D**) Samples stimulated as in (C) were analyzed by flow cytometry for CD25 expression. Each data point represents one independent biological replicate with the SEM and $*p < 0.05$. (**E**) Naive WT, *Nfkbia*$^{NES/NES}$, and *Rel*$^{-/-}$ CD8 T cells were stimulated as in (C) for 48 h and analyzed by flow cytometry for phosphorylated STAT5. (**F**) Naive WT and *Nfkbia*$^{NES/NES}$ CD8 T cells were unstimulated or stimulated with 5 μg/ml each of anti-CD3 and anti-CD28 Abs with control Rat IgG, anti-OX40 Ab (5 μg/ml), or anti-CD27 Ab (5 μg/ml) crosslinked by anti-rat and anti-hamster Ig for 48 h. Supernatants were analyzed by ELISA for IL-2. Data are the mean ± SEM of three technical replicates and $*p < 0.05$ and representative of three independent experiments. (**G**) Samples stimulated as in (F) analyzed by flow cytometry for CD25 expression. Each data point represents one independent biological replicate and SEM is indicated with $*p < 0.05$. (**H**) Naive WT and *Nfkbia*$^{NES/NES}$ CD8 T cells isolated from the spleen were labeled with CFSE and stimulated with 5 μg/ml of anti-CD3 and anti-CD28 Abs along with the indicated concentrations of anti–4-1BB for 72 h. Percentages of undivided cells (right) and divided cells (left) are shown. Data are representative of experiments performed independently at least three times. (**I**) Naive WT and *Nfkbia*$^{NES/NES}$ CD8 T cells were stimulated as in Supplemental Fig. 2F. Absolute live cell numbers were quantified by flow cytometry. Data are representative of experiments performed independently at least three times.

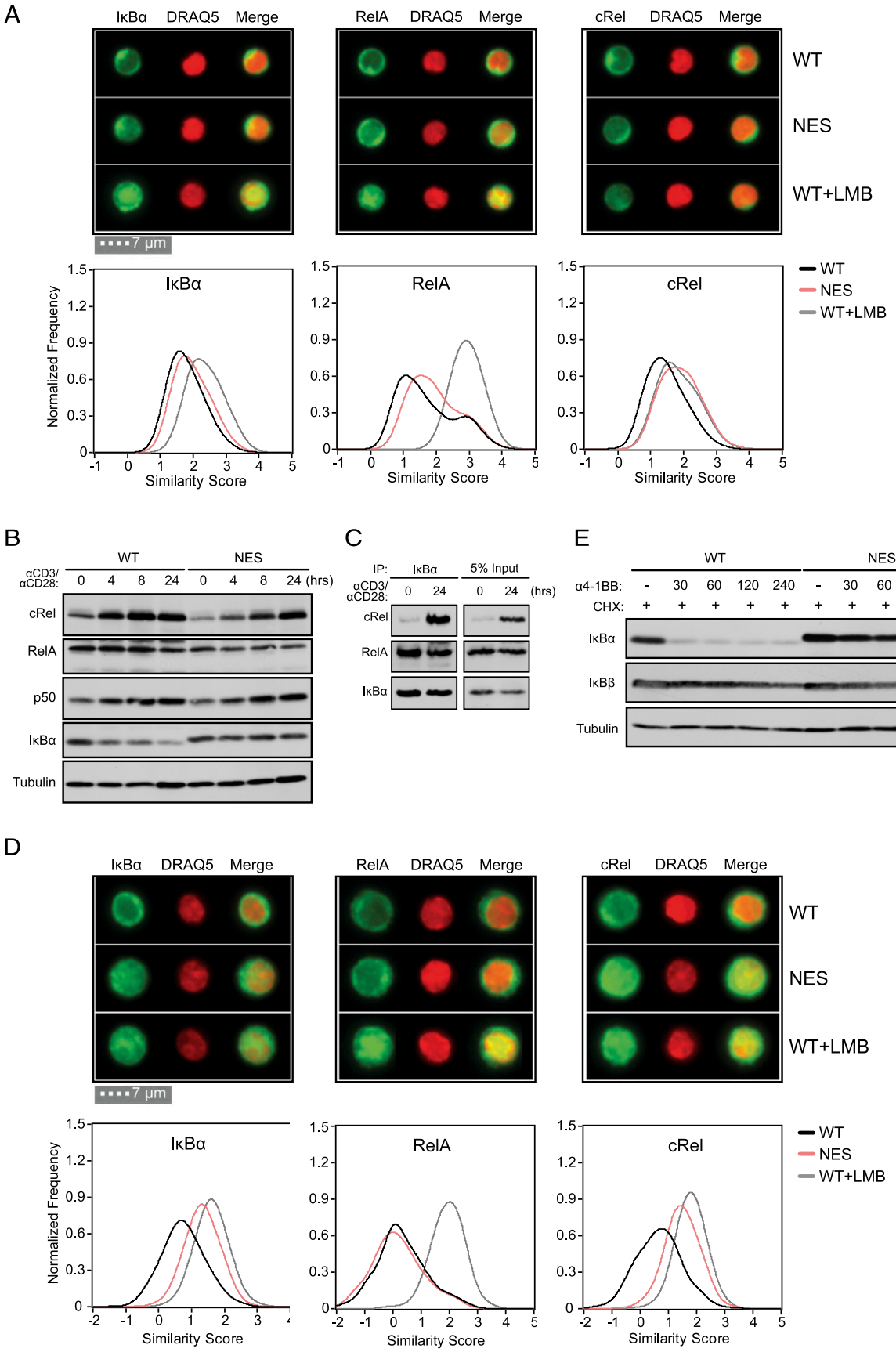

FIGURE 3. IκBα NES is necessary for CD3+CD28 induced cytoplasmic localization of IκBα:cRel complexes to enable efficient 4-1BB signaling. (**A**) Naive WT and *Nfkbia*$^{NES/NES}$ CD8 T cells were fixed, permeabilized, and stained with anti-IκBα, RelA, or cRel Abs and the DRAQ5 nuclear dye. WT cells were treated with 20 ng/ml of LMB for 45 min as a control. Single-cell image analysis by ImageStream flow cytometry. Representative images from each group are shown at an equivalent 60× magnification (above) and the similarity score for each Ab staining is plotted. Data plotted include three independent experiments (see *Materials and Methods*). (**B**) Naive WT and *Nfkbia*$^{NES/NES}$ CD8 T cells were stimulated for the indicated *(Figure legend continues)*

motifs in NES-dependent genes when compared with NES-independent genes, along with less significant enrichment for RelA:p50 and cRel:cRel motifs (Fig. 4F). Despite the fact that a cRel:p50 binding site was not detected in the IL-2 gene by the above bioinformatic analysis, we confirmed cRel binding (16.5-fold over basal) to an NF-κB consensus sequence from the IL-2 gene promoter in WT T cells stimulated with CD3+CD28+4-1BB for 12 h, which was reduced (to 5.2-fold) in *Nfkbia*$^{NES/NES}$ T cells (Supplemental Fig. 2A). RelA binding also increased in CD3+CD28+4-1BB–stimulated WT cells but was much less than cRel binding. These results suggested that 4-1BB stimulation induced a prominent cRel-dependent transcriptional program in CD3+CD28–activated CD8 T cells, which was enabled by IκBα NES–mediated proper subcellular distribution of cRel complexes.

The IκBα NES is necessary for cell-intrinsic antiviral CD8 T cell responses in vivo

These results have thus far demonstrated that CD8 T cells in *Nfkbia*$^{NES/NES}$ mice have 4-1BB–mediated NF-κB signaling, transcriptomic and functional defects ex vivo. To test whether IκBα nuclear export was also necessary for activation and expansion of CD8 T cells in vivo, we used the Armstrong strain of LCMV that induces a well-defined virus-specific T cell response (26). At the peak of the antiviral CD8 T cell response (i.e., day 8 postinfection), the accumulation of activated (CD8 CD44^{hi}) and LCMV NP396–specific CD8 T cells in the spleen of *Nfkbia*$^{NES/NES}$ mice was significantly lower than in WT mice (Fig. 5A). These data suggested that loss of IκBα nuclear export reduced expansion of CD8 T cells during an acute viral infection. Our ex vivo results demonstrated that *Nfkbia*$^{NES/NES}$ CD8 T cells produced significantly lower levels of *Il2* transcript (Fig. 4E) and IL-2 protein (Fig. 2C), and displayed defects in IL-2–dependent survival, following activation (Fig. 2I). To test the hypothesis that a defective production of IL-2 was at least in part responsible for a defect in CD8 T cell accumulation in LCMV-infected *Nfkbia*$^{NES/NES}$ mice in vivo, IL-2 was administered for 6 d following LCMV infection. Although IL-2 administration of LCMV-infected WT mice increased the percentage of CD8 T cells, it did not increase the percentages or the total number of LCMV NP396- or GP33-specific CD8 T cells in the spleen (Fig. 5B, 5C). Strikingly, IL-2 administration completely restored the accumulation of LCMV-specific CD8 T cells in the spleens of *Nfkbia*$^{NES/NES}$ mice (Fig. 5B, 5C). These data suggested that exogenous IL-2 administration could overcome defective accumulation of CD8 T cells in LCMV-infected *Nfkbia*$^{NES/NES}$ mice.

Although our data above demonstrated that virus-specific CD8 T cell responses were suboptimal in *Nfkbia*$^{NES/NES}$ mice and could be restored by exogenous IL-2 administration, this defect could be cell extrinsic because of the presence of the IκBα NES mutation in the germline. Moreover, *Nfkbia*$^{NES/NES}$ mice also harbor B cell and secondary tissue disruptions (25), which might have impacted antiviral CD8 T cell responses. Thus, we further performed three different in vivo studies to address this question. First, to address whether defects in antiviral CD8 T cell responses in *Nfkbia*$^{NES/NES}$ mice originated from hematological cell populations, we generated mixed bone marrow chimeras. Lethally irradiated Ly5.1 host mice were reconstituted with a mix of bone marrow cells from congenically marked host strain (Ly5.1) and Ly5.2 *Nfkbia*$^{WT/WT}$ or *Nfkbia*$^{NES/NES}$ mice, generating control and experimental chimeras (CC and EC, respectively) (Supplemental Fig. 4A). As expected, the *Nfkbia*$^{NES/NES}$ compartment of CC and EC had normal T cell populations (Supplemental Fig. 4B). At day 8 postinfection, we quantified LCMV-specific CD8 T cell responses in control and EC. The activation of WT (Ly5.1$^+$) host CD8 T cell responses were comparable in control and EC; percentages of WT NP396-specific CD8 T cells among Ly5.1$^+$ CD8 T cells were comparable between control and EC (Supplemental Fig. 4C). CD8 T cells derived from *Nfkbia*$^{WT/WT}$ (Ly5.2$^+$) bone marrow cells showed strong activation in control chimeras; >10% of the CD8 T cells were specific to the immunodominant epitope $NP_{396–404}$ (Fig. 6A). By contrast, the percentages of *Nfkbia*$^{NES/NES}$ (Ly5.2) $NP_{396–404}$–specific CD8 T cells in EC were lower, as compared with their Ly5.2 WT counterparts in CC (Fig. 6A). We also calculated the ratios of the percentages of Ly5.1$^+$ to Ly5.2$^+$ NP396-specific CD8 T cells in CCs and ECs. The Ly5.1/Ly5.2 ratio of NP396-specific CD8 T cells in CCs and ECs were 0.83 and 1.72, respectively, and this was statistically significant (p = 0.029). The significant reduction of $NP_{396–404}$–specific cells in the *Nfkbia*$^{NES/NES}$ compartment persisted through the memory phase at 64 d postinfection to a rechallenge with LCMV clone 13 (Supplemental Fig. 4D). These results support the conclusion that the antiviral CD8 T cell defect in *Nfkbia*$^{NES/NES}$ mice was of hematological origin and likely cell intrinsic.

Next, to specifically address whether the above *Nfkbia*$^{NES/NES}$ mouse defects were CD8 T cell–intrinsic, we crossed *Nfkbia*$^{NES/NES}$ mice with LCMV GP 33-specific TCR-transgenic P14 mice to generate P14/*Nfkbia*$^{NES/NES}$ mice. Thy1.1$^+$ hosts were adoptively transferred with either P14/*Nfkbia*$^{WT/WT}$ (Ly5.2$^+$/Thy1.2$^+$) or P14/*Nfkbia*$^{NES/NES}$ (Ly5.2$^+$/Thy1.2$^+$) naive CD8 T cells and then infected with LCMV to test the responses of donor mutant CD8 T cells (Supplemental Fig. 4E, noncompetitive environment). Analysis of mice 8 d postinfection revealed a significantly reduced expansion of P14/*Nfkbia*$^{NES/NES}$ cells in comparison with P14/*Nfkbia*$^{WT/WT}$–transgenic cells (Fig. 6B). Thus, these results indicated that the antiviral CD8 T cell expansion defect of *Nfkbia*$^{NES/NES}$ mice was cell intrinsic. Finally, to further validate this, we performed the same experiment in a competitive environment in which an equal number of P14/*Nfkbia*$^{WT/WT}$ (Ly5.1$^+$/Thy1.2$^+$) and P14/*Nfkbia*$^{NES/NES}$ (Ly5.2$^+$/Thy1.2$^+$) naive CD8 T cells were adoptively transferred into Thy1.1 mice and then infected with LCMV (Supplemental Fig. 4F, competitive environment). Examination of mice after establishment of transferred cells prior to infection showed a slightly higher level of the *Nfkbia*$^{NES/NES}$ CD8 T cells relative to *Nfkbia*$^{WT/WT}$ cells in the hosts (Supplemental Fig. 4F, right). However, at 8 d postinfection, P14/*Nfkbia*$^{NES/NES}$ T cell expansion was significantly reduced in comparison with P14/*Nfkbia*$^{WT/WT}$ cells (Fig. 6C), demonstrating that the *Nfkbia*$^{NES/NES}$ CD8 T cells were unable to effectively compete with *Nfkbia*$^{WT/WT}$ cells in the identical host environment. Our data collectively support the critical role of IκBα NES to promote proper cell-intrinsic antiviral CD8 T cell responses in vivo.

times with 5 μg/ml each anti-CD3 and anti-CD28. Immunoblot analysis of cRel, RelA, p50, IκBα, and tubulin is shown. Data are representative of three independent experiments. (**C**) Cell extracts from naive WT CD8 T cells and those unstimulated or stimulated as in (B) for 24 h were immunoprecipitated with an Ab specific for IκBα. Immunoblot analysis of cRel, RelA, and IκBα is shown. (**D**) Naive WT and *Nfkbia*$^{NES/NES}$ CD8 T cells were stimulated for 24 h with 5 μg/ml each anti-CD3 and anti-CD28 and stained and analyzed as in (A). Representative images for each Ab staining are shown at the equivalent 60× magnification as in (A). Note the larger cell size of the stimulated cells relative to naive cells in (A). (**E**) Naive WT and *Nfkbia*$^{NES/NES}$ CD8 T cells were stimulated for 24 h with anti-CD3 and anti-CD28 Abs as in (A). Following stimulation, cells were pretreated with 20 μg/ml cycloheximide (CHX) for 30 min and then stimulated with 0.05 μg/ml anti–4-1BB Ab for the indicated times. Immunoblot analysis of IκBα, IκBβ, and tubulin is shown.

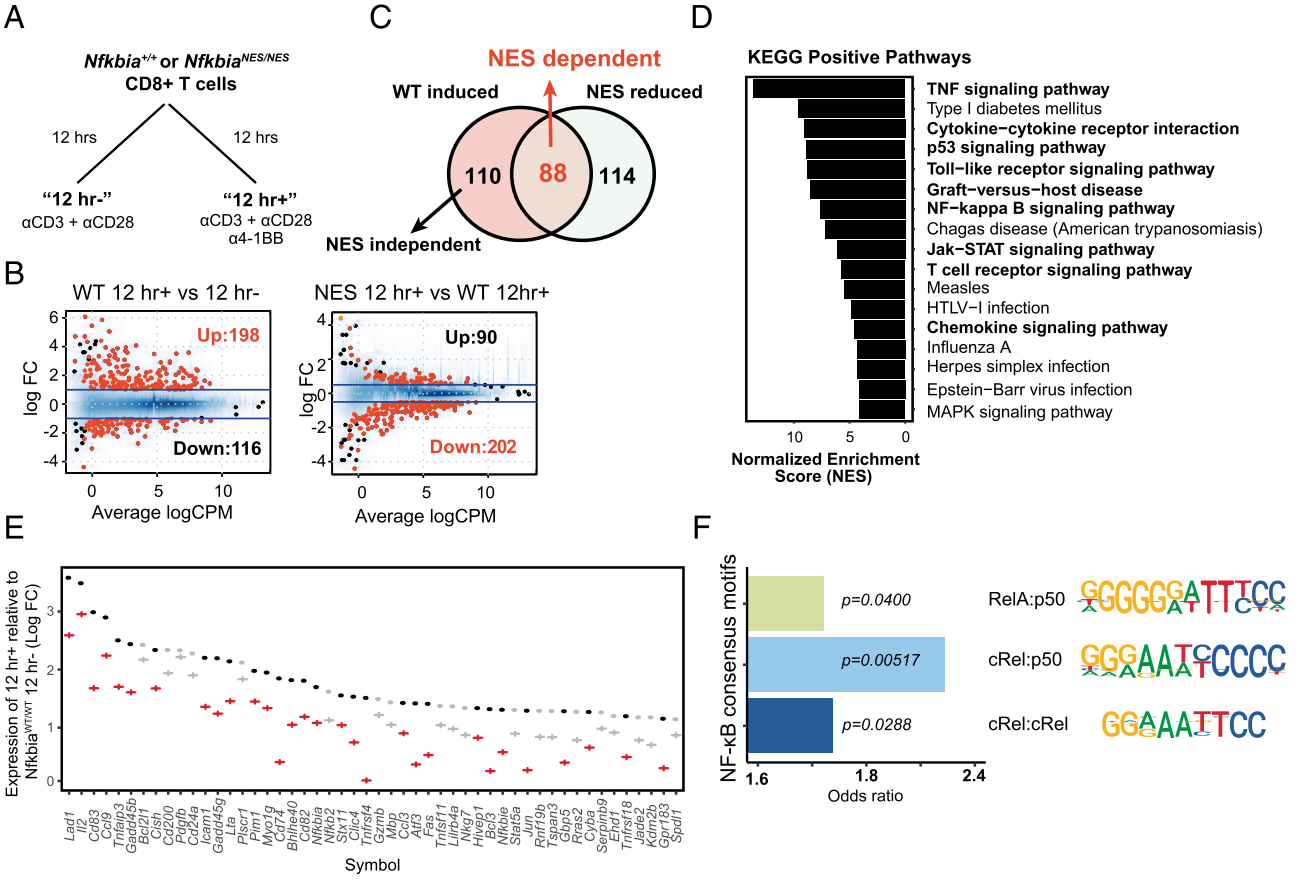

FIGURE 4. IκBα nuclear export is required for inducing a 4-1BB–mediated NF-κB transcriptional program in CD8 T cells. (**A**) The RNA-seq study design is shown with naive *Nfkbia*$^{+/+}$ and *Nfkbia*$^{NES/NES}$ CD8 T cells stimulated with 5 μg/ml each of anti-CD3 and anti-CD28 Abs for 12 h without (12 h−) or with (12 h+) 0.05 μg/ml anti–4-1BB Ab. (**B**) MA plots showing differentially expressed genes (up and down) between "12 h+" versus "12 h−" WT CD8 T cells (left, absolute log2 fold change >1 and FDR <0.01) and between WT "12 h+" versus *Nfkbia*$^{NES/NES}$ "12 h+" (right, absolute log2 fold change >0.5 and FDR <0.05). (**C**) Venn diagram illustrating the number of genes regulated by 4-1BB and by *Nfkbia*$^{NES/NES}$ in CD8 T cells. (**D**) Bar graph showing ranked fold enrichment of enriched Kyoto Encyclopedia of Genes and Genomes pathways (*p* value <0.05) in NES-dependent genes. (**E**) Comparison of expression of the top 20 WT 12 h+ versus 12 h− genes. Dots and crosses represent log2 fold change comparing WT "12 h+" versus WT "12 h−" and *Nfkbia*$^{NES/NES}$ "12 h+" versus WT "12 h−," respectively, with red and gray colors indicating NES dependent and NES independent, respectively. (**F**) Bar graph showing the odds ratios for the occurrence of NF-κB dimer binding motifs (p65:p50, cRel:p50, cRel:cRel) in the promoter regions (−1 kb to 300bp) of NES-dependent genes. The *p* values from the same Fisher exact test are shown.

Discussion

We have now uncovered an unexpected new physiological role for IκBα, as a signal-specific amplifier, not just an inhibitor, of the NF-κB pathway in CD8 T cells, mediated by its unique nuclear export function. Our studies revealed that initial TCR (CD3) and CD28 engagement increased the expression of 4-1BB (and other TNFR superfamily members), increased expression of cRel, and resulted in an upregulation of IκBα:cRel cytosolic complexes. This coordinated receptor and NF-κB pathway reconfiguration sets the stage for 4-1BB–mediated cRel activation because of selective targeting of IκBα degradation by 4-1BB signaling. Sustained cRel activation was dependent on continual IκBα-mediated nuclear export of inactive cRel and was necessary for a dominant cRel transcriptional program, maximal production of IL-2, and primary accumulation of virus-specific CD8 T cells. There was no measurable impact on 4-1BB–induced noncanonical NF-κB signaling by the IκBα NES mutation. Thus, our data suggest a spatial and temporal regulation of canonical NF-κB signaling that is dynamically sustained by IκBα nuclear export to enable optimal CD8 T cell expansion in vivo.

Our findings uncovered aspects of CD8 T cell biology that have not been revealed by previous NF-κB and IκB family member genetic knockout mouse studies (14, 15, 41–48). This study, together with our prior work (25), demonstrated that although there was reduced basal RelA activity and reduced steady-state expression of several NF-κB family members, NES-mutated IκBα has minimal impact on the number of CD4 and CD8 T cell populations in the periphery. CD3+CD28-induced acute RelA and cRel activation, IL-2 secretion, expression of several key cell surface activation markers, and proliferation were all normal in *Nfkbia*$^{NES/NES}$ CD8 T cells. The lack of an acute RelA activation defect in naive *Nfkbia*$^{NES/NES}$ CD8 T cells is likely a consequence of the presence of a compensating NES on RelA. In contrast, the lack of an acute CD3+CD28-induced cRel activation defect in naive *Nfkbia*$^{NES/NES}$ CD8 T cells is likely due to the primary association of cRel with IκBβ, not mutant IκBα, in naive T cells (24, 49). A minor level of cRel associated with IκBα in naive *Nfkbia*$^{NES/NES}$ cells appears to be subjected to alteration in subcellular localization detected by ImageStream flow cytometry. However, this fraction of cRel and IκBα is too small to have a major impact on acute CD3+CD28-induced signaling in naive cells. In contrast, cRel becomes highly susceptible to IκBα nuclear export–mediated regulation after increased cRel synthesis and subsequent increased cRel:IκBα complex formation following CD3+CD28 stimulation. Because cRel does not have its own NES sequence and function, its subcellular localization is dominantly

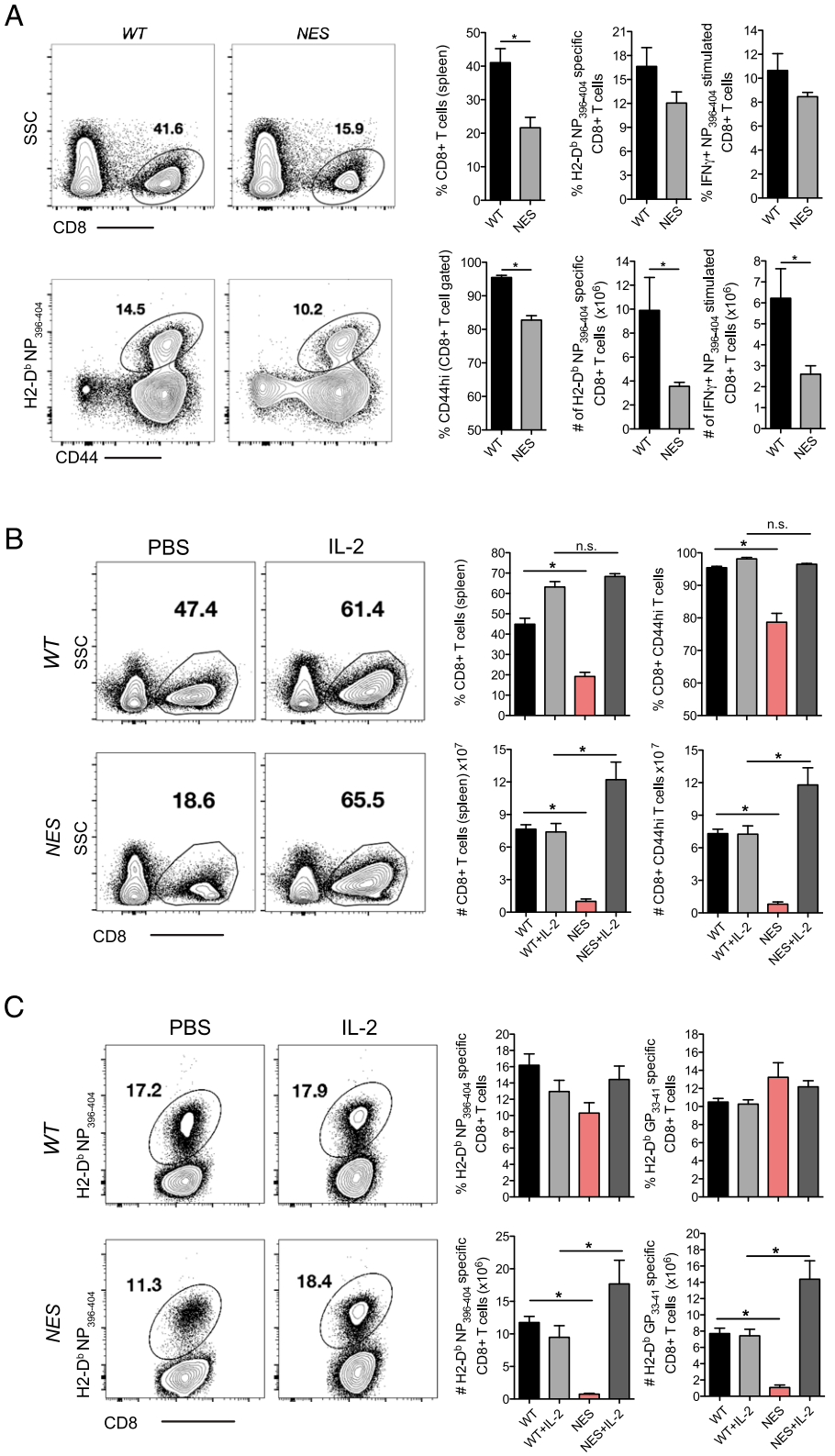

FIGURE 5. *Nfkbia*$^{NES/NES}$ mice have a primary CD8 T cell expansion defect following LCMV infection, which can be restored by exogenous IL-2 administration. (**A**) WT and *Nfkbia*$^{NES/NES}$ mice were infected with LCMV Armstrong. Eight days postinfection, splenocytes from each group were assessed by flow cytometry for CD8 T cells staining positive for CD44 and H2-D^b–specific NP$_{396–404}$ tetramer and staining positive for IFN-γ following restimulation with NP$_{396–404}$ peptide. (**B**) WT and *Nfkbia*$^{NES/NES}$ mice were infected with LCMV Armstrong. Mice were injected with recombinant human IL-2 (10,000 IU) or PBS twice a day for 6 d following infection. Eight days postinfection, splenocytes were analyzed by flow cytometry and percentages and absolute numbers of cells staining positive for CD8 and CD44 are shown. (**C**) WT and *Nfkbia*$^{NES/NES}$ mice from (B) were also analyzed by flow cytometry with percentages and absolute numbers staining positive for GP$_{33–41}$ and NP$_{396–404}$ tetramers shown. Data shown in (A)–(C) are the mean ± SEM of five mice per group and representative of two independent experiments with $*p < 0.05$.

controlled by IκBα. Thus, we now show that the major physiological role of IκBα NES is realized primarily when the fraction of cRel:IκBα complexes increase significantly following TCR+CD28 stimulation in CD8 T cells.

How TNFR family members coordinate their expression and cell signaling processes to functional transcriptional programs has remained undefined (50). 4-1BB expression is itself known to be regulated by NF-κB signaling following T cell signaling (51); however, *Nfkbia*$^{NES/NES}$ CD8 T cells set the same stage with coordinated expression of 4-1BB and cRel as in WT cells following CD3+CD28 stimulation. Consequently, in WT cells, cRel complexes are potently activated by subsequent 4-1BB signaling due to the selective degradation of IκBα over IκBβ, followed by a 4-1BB–dependent transcriptional program, heightened IL-2 production and

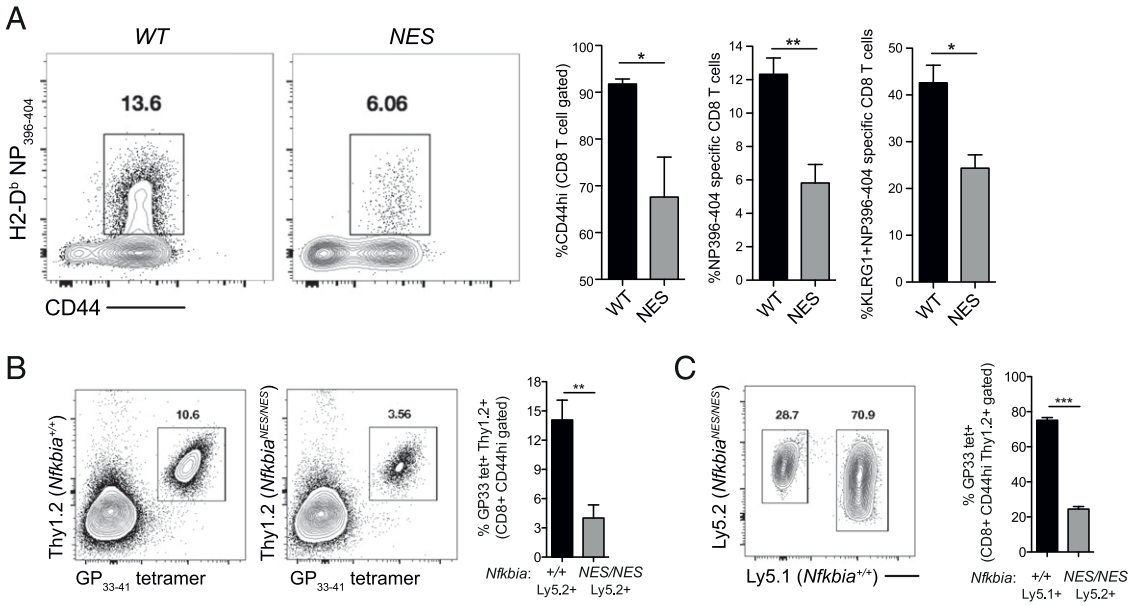

FIGURE 6. The antiviral defect in *Nfkbia*$^{NES/NES}$ mice is CD8 T cell–intrinsic. (**A**) Lethally irradiated Ly5.1 host mice were reconstituted with a mix of bone marrow to generate CC (Ly5.1$^+$ host strain cells and Ly5.2$^+$ *Nfkbia*$^{WT/WT}$) or EC (Ly5.1$^+$ host strain cells and Ly5.2$^+$ *Nfkbia*$^{NES/NES}$) (see Supplemental Fig. 4A for schematic) and infected with LCMV Armstrong. Eight days postinfection, splenocytes from CC and EC were assessed by flow cytometry for Ly5.2$^+$ CD8 T cells staining positive for CD44, CD62L, $NP_{396–404}$ tetramer, and KLRG1. Data are the mean ± SEM and representative of three to four mice per group with statistical significance at $*p < 0.05$, $**p < 0.01$. (**B**) Thy1.1 host mice were adoptively transferred with either P14-transgenic Thy1.2$^+$ *Nfkbia*$^{WT/WT}$ (Ly5.2$^+$) or P14-transgenic Thy1.2$^+$ *Nfkbia*$^{NES/NES}$ (Ly5.2$^+$) CD8 T cells. Mice were infected with LCMV Armstrong and analyzed 8 d postinfection for P14-transgenic T cell expansion. Data are the mean ± SEM and representative of six mice per group with statistical significance at $**p < 0.01$. (**C**) Thy1.1 host mice were adoptively transferred with a 1:1 mix of P14-transgenic Thy1.2$^+$ *Nfkbia*$^{+/+}$ (Ly5.1$^+$) and Thy1.2$^+$ *Nfkbia*$^{NES/NES}$ (Ly5.2$^+$) cells. Twenty-four hours later, mice were infected with LCMV Armstrong and analyzed 8 d postinfection for P14 transgenic T cell expansion. Data are the mean ± SEM and representative of seven mice per group with statistical significance at $***p < 0.001$.

cell proliferation. In contrast, in *Nfkbia*$^{NES/NES}$ CD8 T cells, because of defective localization of cRel:IκBα complexes to the nucleus, which shields them from 4-1BB-induced signaling, the chain of events necessary for IL-2 production and activation is disrupted. Our data further suggested that such 4-1BB regulation is not unique to this TNFR family member but is also likely shared by OX40 and CD27. Thus, IκBα-mediated nuclear export of cRel ensures a spatial regulation of NF-κB dimers, particularly cRel dimers, to sustain the TNFR costimulatory signaling necessary for proper T cell immunity.

Of the many genes whose expression is altered by the IκBα NES mutation in CD8 T cells, IL-2 appears to be one of the most critical cytokines that controls their accumulation in response to viral infection. On first glance, this appears unsurprising given 1) the significant inhibition of cRel dimer activity in *Nfkbia*$^{NES/NES}$ CD8 T cells and 2) the fact that *Rel*$^{-/-}$ T cells have an IL-2 synthesis defect and fail to proliferate in vitro (14, 15). However, despite the significant reduction of 4-1BB–induced IL-2 secretion, *Nfkbia*$^{NES/NES}$ CD8 T cells proliferated surprisingly normally in vitro, making it distinct from the total cRel-deficient T cell phenotype. In contrast, withdrawal of TCR and costimulatory signals revealed that *Nfkbia*$^{NES/NES}$ CD8 T cells depended on autocrine IL-2 secretion to sustain survival in vitro. This suggests the possibility that TCR and costimulatory signals trigger a program of CD8 T cell expansion that is dependent on autocrine IL-2 even after exogenous stimuli are removed. Previous studies have suggested that depending on the route or model of infection, autocrine IL-2 is necessary for expansion of viral-specific CD8 T cells (52–54); however, how autocrine IL-2 is regulated in activated CD8 T cells in vivo remained unclear. Our biochemical and transcriptomic analyses demonstrated that the nuclear export function of IκBα assumes an unexpectedly significant cell autonomous role in the regulation of cRel dimer activity to likely maintain autocrine IL-2 production. Similar to a previously published study investigating the role of IL-2 in effector differentiation (55), a significant reduction in KLRG1^{hi} *Nfkbia*$^{NES/NES}$ CD8 T cells provided evidence that IL-2 production was defective following LCMV infection. Thus, whereas other aspects of CD8 T cell function may require additional factors, the ability of exogenous IL-2 to restore CD8 T cell accumulation defects in LCMV-infected *Nfkbia*$^{NES/NES}$ mice, coupled with chimera and adoptive transfer studies showing CD8 T cell–intrinsic defects, supports the biological significance of autocrine IL-2 production by CD8 T cells in vivo. Also, it shows that defects in autocrine IL-2 production by CD8 T cells can be overcome by supraphysiological levels of exogenous IL-2.

The newly uncovered role of nuclear export-dependent regulation of CD8 T cell immunity may have implications beyond antiviral responses. Exportin-1/chromosome region maintenance 1 (XPO1/CRM1) mediates the nuclear export of classical NES-containing proteins, including IκBα and RelA. Many tumors overexpress XPO1, and pharmacologic inhibition of XPO1-mediated nuclear export can result in tumor cell death or sensitivity to chemotherapies (56). Recently, usage of selective inhibitors of nuclear export compounds have been shown to be tolerated in clinical trials for treatment of hematologic and solid tumors (57). However, thorough mechanistic studies investigating the physiological consequences of nuclear export inhibition in the immune system are lacking. To our knowledge, the *Nfkbia*$^{NES/NES}$ mouse represents one of only two genetically modified mouse models to reveal insights into the physiological role of nuclear export in vivo (25, 58). Given the increased focus on the significance of antitumor CD8 T cell immune responses and use of chimeric Ag receptor T cells containing 4-1BB signaling domains (59), our study provides significant aspects of CD8 T cell biology that may be

considered to improve antitumor immunity and chimeric Ag receptor T cell strategies, including timing of the administration of selective inhibitors of nuclear export compounds with immunotherapy approaches (60).

Collectively, our study has provided new insights into how CD8 T cell immunity is dependent on the coordinated reconfiguration of an intracellular signaling system and cognate cell surface receptors to enable signaling through costimulatory receptors. Although it is well appreciated that fine adjustments of extracellular physical interactions, such as Ag-receptor and ligand-receptor interactions, govern one part of T cell function (61), to our knowledge, our study uncovered that regulation of intracellular cell signaling dynamics is another critical point of regulation. We now provide a plausible model that links dynamic CD8 T cell signaling through nuclear export of specific NF-κB family members to three key events in CD8 T cell immunity in vivo: sustained signaling through costimulatory TNFR members, autocrine IL-2 production, and maximal accumulation of effector cells.

Acknowledgments

We thank the University of Wisconsin Carbone Cancer Center Flow Cytometry Core Facility, the National Institutes of Health Tetramer Core Facility (Atlanta, GA) for H-2D(b)/KAVYNFATM and H-2D(b)/FQPQNGQFI tetramers, the University of Wisconsin-Madison Biomedical Research Model Services Mouse Breeding Core for mouse colony maintenance, Dr. Hsiou-Chi Liou for *Rel*$^{-/-}$ mice, Dr. Rafi Ahmed for P14 TCR-transgenic mice, and members of the Miyamoto laboratory for thoughtful discussions.

Disclosures

The authors have no financial conflicts of interest.

References

1. Duttagupta, P. A., A. C. Boesteanu, and P. D. Katsikis. 2009. Costimulation signals for memory CD8+ T cells during viral infections. *Crit. Rev. Immunol.* 29: 469–486.
2. Croft, M. 2009. The role of TNF superfamily members in T-cell function and diseases. *Nat. Rev. Immunol.* 9: 271–285.
3. Jameson, S. C., and D. Masopust. 2009. Diversity in T cell memory: an embarrassment of riches. *Immunity* 31: 859–871.
4. Chen, L., and D. B. Flies. 2013. Molecular mechanisms of T cell co-stimulation and co-inhibition. [Published erratum appears in 2013 Nat. Rev. Immunol. 13: 542.] *Nat. Rev. Immunol.* 13: 227–242.
5. Borowski, A. B., A. C. Boesteanu, Y. M. Mueller, C. Carafides, D. J. Topham, J. D. Altman, S. R. Jennings, and P. D. Katsikis. 2007. Memory CD8+ T cells require CD28 costimulation. *J. Immunol.* 179: 6494–6503.
6. Wortzman, M. E., D. L. Clouthier, A. J. McPherson, G. H. Lin, and T. H. Watts. 2013. The contextual role of TNFR family members in CD8(+) T-cell control of viral infections. *Immunol. Rev.* 255: 125–148.
7. Oeckinghaus, A., M. S. Hayden, and S. Ghosh. 2011. Crosstalk in NF-κB signaling pathways. *Nat. Immunol.* 12: 695–708.
8. Hayden, M. S., and S. Ghosh. 2011. NF-κB in immunobiology. *Cell Res.* 21: 223–244.
9. Napetschnig, J., and H. Wu. 2013. Molecular basis of NF-κB signaling. *Annu. Rev. Biophys.* 42: 443–468.
10. Dobrzanski, P., R. P. Ryseck, and R. Bravo. 1994. Differential interactions of Rel-NF-kappa B complexes with I kappa B alpha determine pools of constitutive and inducible NF-kappa B activity. *EMBO J.* 13: 4608–4616.
11. Gerondakis, S., and U. Siebenlist. 2010. Roles of the NF-kappaB pathway in lymphocyte development and function. *Cold Spring Harb. Perspect. Biol.* 2: a000182.
12. Beg, A. A., W. C. Sha, R. T. Bronson, S. Ghosh, and D. Baltimore. 1995. Embryonic lethality and liver degeneration in mice lacking the RelA component of NF-kappa B. *Nature* 376: 167–170.
13. Oh, H., Y. Grinberg-Bleyer, W. Liao, D. Maloney, P. Wang, Z. Wu, J. Wang, D. M. Bhatt, N. Heise, R. M. Schmid, et al. 2017. An NF-κB transcription-factor-dependent lineage-specific transcriptional program promotes regulatory T cell identity and function. *Immunity* 47: 450–465.e5.
14. Doi, T. S., T. Takahashi, O. Taguchi, T. Azuma, and Y. Obata. 1997. NF-kappa B RelA-deficient lymphocytes: normal development of T cells and B cells, impaired production of IgA and IgG1 and reduced proliferative responses. *J. Exp. Med.* 185: 953–961.
15. Köntgen, F., R. J. Grumont, A. Strasser, D. Metcalf, R. Li, D. Tarlinton, and S. Gerondakis. 1995. Mice lacking the c-rel proto-oncogene exhibit defects in lymphocyte proliferation, humoral immunity, and interleukin-2 expression. *Genes Dev.* 9: 1965–1977.
16. Sun, S. C., P. A. Ganchi, D. W. Ballard, and W. C. Greene. 1993. NF-kappa B controls expression of inhibitor I kappa B alpha: evidence for an inducible autoregulatory pathway. *Science* 259: 1912–1915.
17. Chiao, P. J., S. Miyamoto, and I. M. Verma. 1994. Autoregulation of I kappa B alpha activity. *Proc. Natl. Acad. Sci. USA* 91: 28–32.
18. Huang, T. T., N. Kudo, M. Yoshida, and S. Miyamoto. 2000. A nuclear export signal in the N-terminal regulatory domain of IkappaBalpha controls cytoplasmic localization of inactive NF-kappaB/IkappaBalpha complexes. *Proc. Natl. Acad. Sci. USA* 97: 1014–1019.
19. Huang, T. T., and S. Miyamoto. 2001. Postrepression activation of NF-kappaB requires the amino-terminal nuclear export signal specific to IkappaBalpha. *Mol. Cell. Biol.* 21: 4737–4747.
20. Johnson, C., D. Van Antwerp, and T. J. Hope. 1999. An N-terminal nuclear export signal is required for the nucleocytoplasmic shuttling of IkappaBalpha. *EMBO J.* 18: 6682–6693.
21. Tam, W. F., L. H. Lee, L. Davis, and R. Sen. 2000. Cytoplasmic sequestration of rel proteins by IkappaBalpha requires CRM1-dependent nuclear export. *Mol. Cell. Biol.* 20: 2269–2284.
22. Tam, W. F., and R. Sen. 2001. IkappaB family members function by different mechanisms. *J. Biol. Chem.* 276: 7701–7704.
23. Harhaj, E. W., and S. C. Sun. 1999. Regulation of RelA subcellular localization by a putative nuclear export signal and p50. *Mol. Cell. Biol.* 19: 7088–7095.
24. Tam, W. F., W. Wang, and R. Sen. 2001. Cell-specific association and shuttling of IkappaBalpha provides a mechanism for nuclear NF-kappaB in B lymphocytes. *Mol. Cell. Biol.* 21: 4837–4846.
25. Wuerzberger-Davis, S. M., Y. Chen, D. T. Yang, J. D. Kearns, P. W. Bates, C. Lynch, N. C. Ladell, M. Yu, A. Podd, H. Zeng, et al. 2011. Nuclear export of the NF-κB inhibitor IκBα is required for proper B cell and secondary lymphoid tissue formation. *Immunity* 34: 188–200.
26. Ahmed, R., A. Salmi, L. D. Butler, J. M. Chiller, and M. B. Oldstone. 1984. Selection of genetic variants of lymphocytic choriomeningitis virus in spleens of persistently infected mice. Role in suppression of cytotoxic T lymphocyte response and viral persistence. *J. Exp. Med.* 160: 521–540.
27. Murali-Krishna, K., J. D. Altman, M. Suresh, D. J. Sourdive, A. J. Zajac, J. D. Miller, J. Slansky, and R. Ahmed. 1998. Counting antigen-specific CD8 T cells: a reevaluation of bystander activation during viral infection. *Immunity* 8: 177–187.
28. O'Riordan, K. J., I. C. Huang, M. Pizzi, P. Spano, F. Boroni, R. Egli, P. Desai, O. Fitch, L. Malone, H. J. Ahn, et al. 2006. Regulation of nuclear factor kappaB in the hippocampus by group I metabotropic glutamate receptors. *J. Neurosci.* 26: 4870–4879.
29. Dobin, A., C. A. Davis, F. Schlesinger, J. Drenkow, C. Zaleski, S. Jha, P. Batut, M. Chaisson, and T. R. Gingeras. 2013. STAR: ultrafast universal RNA-seq aligner. *Bioinformatics* 29: 15–21.
30. Liao, Y., G. K. Smyth, and W. Shi. 2014. featureCounts: an efficient general purpose program for assigning sequence reads to genomic features. *Bioinformatics* 30: 923–930.
31. Robinson, M. D., D. J. McCarthy, and G. K. Smyth. 2010. edgeR: a Bioconductor package for differential expression analysis of digital gene expression data. *Bioinformatics* 26: 139–140.
32. Alves, B. N., R. Tsui, J. Almaden, M. N. Shokhirev, J. Davis-Turak, J. Fujimoto, H. Birnbaum, J. Ponomarenko, and A. Hoffmann. 2014. IκBε is a key regulator of B cell expansion by providing negative feedback on cRel and RelA in a stimulus-specific manner. *J. Immunol.* 192: 3121–3132.
33. Siggers, T., A. B. Chang, A. Teixeira, D. Wong, K. J. Williams, B. Ahmed, J. Ragoussis, I. A. Udalova, S. T. Smale, and M. L. Bulyk. 2011. Principles of dimer-specific gene regulation revealed by a comprehensive characterization of NF-κB family DNA binding. *Nat. Immunol.* 13: 95–102.
34. Heinz, S., C. Benner, N. Spann, E. Bertolino, Y. C. Lin, P. Laslo, J. X. Cheng, C. Murre, H. Singh, and C. K. Glass. 2010. Simple combinations of lineage-determining transcription factors prime cis-regulatory elements required for macrophage and B cell identities. *Mol. Cell* 38: 576–589.
35. Tan, J. T., J. K. Whitmire, R. Ahmed, T. C. Pearson, and C. P. Larsen. 1999. 4-1BB ligand, a member of the TNF family, is important for the generation of antiviral CD8 T cell responses. *J. Immunol.* 163: 4859–4868.
36. Sun, S. C. 2017. The non-canonical NF-κB pathway in immunity and inflammation. *Nat. Rev. Immunol.* 17: 545–558.
37. Nakajima, H., X. W. Liu, A. Wynshaw-Boris, L. A. Rosenthal, K. Imada, D. S. Finbloom, L. Hennighausen, and W. J. Leonard. 1997. An indirect effect of Stat5a in IL-2-induced proliferation: a critical role for Stat5a in IL-2-mediated IL-2 receptor alpha chain induction. *Immunity* 7: 691–701.
38. Kaech, S. M., and R. Ahmed. 2001. Memory CD8+ T cell differentiation: initial antigen encounter triggers a developmental program in naïve cells. *Nat. Immunol.* 2: 415–422.
39. Maguire, O., C. Collins, K. O'Loughlin, J. Miecznikowski, and H. Minderman. 2011. Quantifying nuclear p65 as a parameter for NF-κB activation: correlation between ImageStream cytometry, microscopy, and Western blot. *Cytometry A* 79: 461–469.
40. Wolff, B., J. J. Sanglier, and Y. Wang. 1997. Leptomycin B is an inhibitor of nuclear export: inhibition of nucleo-cytoplasmic translocation of the human immunodeficiency virus type 1 (HIV-1) Rev protein and Rev-dependent mRNA. *Chem. Biol.* 4: 139–147.
41. Franzoso, G., L. Carlson, L. Poljak, E. W. Shores, S. Epstein, A. Leonardi, A. Grinberg, T. Tran, T. Scharton-Kersten, M. Anver, et al. 1998. Mice deficient in nuclear factor (NF)-kappa B/p52 present with defects in humoral responses, germinal center reactions, and splenic microarchitecture. *J. Exp. Med.* 187: 147–159.

42. Alcamo, E., N. Hacohen, L. C. Schulte, P. D. Rennert, R. O. Hynes, and D. Baltimore. 2002. Requirement for the NF-kappaB family member RelA in the development of secondary lymphoid organs. *J. Exp. Med.* 195: 233–244.
43. Weih, F., D. Carrasco, S. K. Durham, D. S. Barton, C. A. Rizzo, R. P. Ryseck, S. A. Lira, and R. Bravo. 1995. Multiorgan inflammation and hematopoietic abnormalities in mice with a targeted disruption of RelB, a member of the NF-kappa B/Rel family. *Cell* 80: 331–340.
44. Guerin, S., M. L. Baron, R. Valero, M. Herrant, P. Auberger, and P. Naquet. 2002. RelB reduces thymocyte apoptosis and regulates terminal thymocyte maturation. *Eur. J. Immunol.* 32: 1–9.
45. Das, J., C. H. Chen, L. Yang, L. Cohn, P. Ray, and A. Ray. 2001. A critical role for NF-kappa B in GATA3 expression and TH2 differentiation in allergic airway inflammation. *Nat. Immunol.* 2: 45–50.
46. Beg, A. A., W. C. Sha, R. T. Bronson, and D. Baltimore. 1995. Constitutive NF-kappa B activation, enhanced granulopoiesis, and neonatal lethality in I kappa B alpha-deficient mice. *Genes Dev.* 9: 2736–2746.
47. Boothby, M. R., A. L. Mora, D. C. Scherer, J. A. Brockman, and D. W. Ballard. 1997. Perturbation of the T lymphocyte lineage in transgenic mice expressing a constitutive repressor of nuclear factor (NF)-kappaB. *J. Exp. Med.* 185: 1897–1907.
48. Rao, P., M. S. Hayden, M. Long, M. L. Scott, A. P. West, D. Zhang, A. Oeckinghaus, C. Lynch, A. Hoffmann, D. Baltimore, and S. Ghosh. 2010. IkappaBbeta acts to inhibit and activate gene expression during the inflammatory response. *Nature* 466: 1115–1119.
49. Banerjee, D., H. C. Liou, and R. Sen. 2005. c-Rel-dependent priming of naive T cells by inflammatory cytokines. *Immunity* 23: 445–458.
50. Mbanwi, A. N., and T. H. Watts. 2014. Costimulatory TNFR family members in control of viral infection: outstanding questions. *Semin. Immunol.* 26: 210–219.
51. Kim, J. O., H. W. Kim, K. M. Baek, and C. Y. Kang. 2003. NF-kappaB and AP-1 regulate activation-dependent CD137 (4-1BB) expression in T cells. *FEBS Lett.* 541: 163–170.
52. Boyman, O., J. H. Cho, and J. Sprent. 2010. The role of interleukin-2 in memory CD8 cell differentiation. *Adv. Exp. Med. Biol.* 684: 28–41.
53. Feau, S., R. Arens, S. Togher, and S. P. Schoenberger. 2011. Autocrine IL-2 is required for secondary population expansion of CD8(+) memory T cells. *Nat. Immunol.* 12: 908–913.
54. Williams, M. A., A. J. Tyznik, and M. J. Bevan. 2006. Interleukin-2 signals during priming are required for secondary expansion of CD8+ memory T cells. *Nature* 441: 890–893.
55. Kalia, V., S. Sarkar, S. Subramaniam, W. N. Haining, K. A. Smith, and R. Ahmed. 2010. Prolonged interleukin-2Ralpha expression on virus-specific CD8+ T cells favors terminal-effector differentiation in vivo. *Immunity* 32: 91–103.
56. Kim, J., E. McMillan, H. S. Kim, N. Venkateswaran, G. Makkar, J. Rodriguez-Canales, P. Villalobos, J. E. Neggers, S. Mendiratta, S. Wei, et al. 2016. XPO1-dependent nuclear export is a druggable vulnerability in KRAS-mutant lung cancer. *Nature* 538: 114–117.
57. Senapedis, W. T., E. Baloglu, and Y. Landesman. 2014. Clinical translation of nuclear export inhibitors in cancer. *Semin. Cancer Biol.* 27: 74–86.
58. Biondi, C. A., D. Das, M. Howell, A. Islam, E. K. Bikoff, C. S. Hill, and E. J. Robertson. 2007. Mice develop normally in the absence of Smad4 nucleocytoplasmic shuttling. *Biochem. J.* 404: 235–245.
59. Long, A. H., W. M. Haso, J. F. Shern, K. M. Wanhainen, M. Murgai, M. Ingaramo, J. P. Smith, A. J. Walker, M. E. Kohler, V. R. Venkateshwara, et al. 2015. 4-1BB costimulation ameliorates T cell exhaustion induced by tonic signaling of chimeric antigen receptors. *Nat. Med.* 21: 581–590.
60. Tyler, P. M., M. M. Servos, R. C. de Vries, B. Klebanov, T. Kashyap, S. Sacham, Y. Landesman, M. Dougan, and S. K. Dougan. 2017. Clinical dosing regimen of selinexor maintains normal immune homeostasis and T-cell effector function in mice: implications for combination with immunotherapy. *Mol. Cancer Ther.* 16: 428–439.
61. Malissen, B., and P. Bongrand. 2015. Early T cell activation: integrating biochemical, structural, and biophysical cues. *Annu. Rev. Immunol.* 33: 539–561.